



HAL
open science

Enhanced Selectivity of the Separation of CO₂ from N₂ during Crystallization of Semi-Clathrates from Quaternary Ammonium Solutions

Jean-Michel Herri, Amina Bouchemoua, Matthias Kwaterski, Pedro Brântuas, Aurélie Galfré, Baptiste Bouillot, Jérôme Douzet, Yamina Ouabbas, Ana Alexandra Cameirao

► To cite this version:

Jean-Michel Herri, Amina Bouchemoua, Matthias Kwaterski, Pedro Brântuas, Aurélie Galfré, et al.. Enhanced Selectivity of the Separation of CO₂ from N₂ during Crystallization of Semi-Clathrates from Quaternary Ammonium Solutions. *Oil & Gas Science and Technology - Revue d'IFP Energies nouvelles*, 2014, 69 (5), pp.947-968. 10.2516/ogst/2013201 . hal-01088706

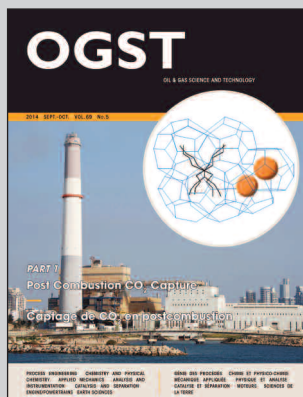
HAL Id: hal-01088706

<https://hal.science/hal-01088706>

Submitted on 23 Nov 2018

HAL is a multi-disciplinary open access archive for the deposit and dissemination of scientific research documents, whether they are published or not. The documents may come from teaching and research institutions in France or abroad, or from public or private research centers.

L'archive ouverte pluridisciplinaire **HAL**, est destinée au dépôt et à la diffusion de documents scientifiques de niveau recherche, publiés ou non, émanant des établissements d'enseignement et de recherche français ou étrangers, des laboratoires publics ou privés.



This paper is a part of the hereunder thematic dossier published in OGST Journal, Vol. 69, No. 5, pp. 773-969 and available online [here](#)

Cet article fait partie du dossier thématique ci-dessous publié dans la revue OGST, Vol. 69, n°5, pp. 773-969 et téléchargeable [ici](#)

DOSSIER Edited by/Sous la direction de : **P.-L. Carrette**

PART 1

Post Combustion CO₂ Capture Captage de CO₂ en postcombustion

Oil & Gas Science and Technology – Rev. IFP Energies nouvelles, Vol. 69 (2014), No. 5, pp. 773-969

Copyright © 2014, IFP Energies nouvelles

- 773 > Editorial
- 785 > *CO₂ Capture Rate Sensitivity Versus Purchase of CO₂ Quotas. Optimizing Investment Choice for Electricity Sector*
Sensibilité du taux de captage de CO₂ au prix du quota européen. Usage du faible prix de quota européen de CO₂ comme effet de levier pour lancer le déploiement de la technologie de captage en postcombustion
P. Coussy and L. Raynal
- 793 > *Emissions to the Atmosphere from Amine-Based Post-Combustion CO₂ Capture Plant – Regulatory Aspects*
Émissions atmosphériques des installations de captage de CO₂ en postcombustion par les amines – Aspects réglementaires
M. Azzi, D. Angove, N. Dave, S. Day, T. Do, P. Feron, S. Sharma, M. Attalla and M. Abu Zahra
- 805 > *Formation and Destruction of NDELA in 30 wt% MEA (Monoethanolamine) and 50 wt% DEA (Diethanolamine) Solutions*
Formation et destruction de NDELA dans des solutions de 30% de MEA (monoéthanolamine) et de 50% de DEA (diéthanolamine)
H. Knuutila, N. Asif, S. J. Vevelstad and H. F. Svendsen
- 821 > *Validation of a Liquid Chromatography Tandem Mass Spectrometry Method for Targeted Degradation Compounds of Ethanolamine Used in CO₂ Capture: Application to Real Samples*
Validation d'une méthode de chromatographie en phase liquide couplée à la spectrométrie de masse en tandem pour des composés de dégradation ciblés de l'éthanolamine utilisée dans le captage du CO₂ : application à des échantillons réels
V. Cuzuel, J. Brunet, A. Rey, J. Dugay, J. Vial, V. Pichon and P.-L. Carrette
- 833 > *Equilibrium and Transport Properties of Primary, Secondary and Tertiary Amines by Molecular Simulation*
Propriétés d'équilibre et de transport d'amines primaires, secondaires et tertiaires par simulation moléculaire
G. A. Orozco, C. Nieto-Draghi, A. D. Mackie and V. Lachet
- 851 > *CO₂ Absorption by Biphasic Solvents: Comparison with Lower Phase Alone*
Absorption du CO₂ par des solvants biphasiques : comparaison avec la phase inférieure isolée
Z. Xu, S. Wang, G. Qi, J. Liu, B. Zhao and C. Chen
- 865 > *Kinetics of Carbon Dioxide with Amines – I. Stopped-Flow Studies in Aqueous Solutions. A Review*
Cinétique du dioxyde de carbone avec les amines – I. Étude par stopped-flow en solution aqueuse. Une revue
G. Couchaux, D. Barth, M. Jacquin, A. Faraj and J. Grandjean
- 885 > *Modeling of the CO₂ Absorption in a Wetted Wall Column by Piperazine Solutions*
Modélisation de l'absorption de CO₂ par des solutions de pipérazine dans un film tombant
A. Servia, N. Laloue, J. Grandjean, S. Rode and C. Roizard
- 903 > *Piperazine/N-methylpiperazine/N,N'-dimethylpiperazine as an Aqueous Solvent for Carbon Dioxide Capture*
Mélange pipérazine/N-méthylpipérazine/N,N'-diméthylpipérazine en solution aqueuse pour le captage du CO₂
S. A. Freeman, X. Chen, T. Nguyen, H. Rafique, Q. Xu and G. T. Rochelle
- 915 > *Corrosion in CO₂ Post-Combustion Capture with Alkanolamines – A Review*
Corrosion dans les procédés utilisant des alcanolamines pour le captage du CO₂ en postcombustion
J. Kittel and S. Gonzalez
- 931 > *Aqueous Ammonia (NH₃) Based Post-Combustion CO₂ Capture: A Review*
Captage de CO₂ en postcombustion par l'ammoniac en solution aqueuse (NH₃) : synthèse
N. Yang, H. Yu, L. Li, D. Xu, W. Han and P. Feron
- 947 > *Enhanced Selectivity of the Separation of CO₂ from N₂ during Crystallization of Semi-Clathrates from Quaternary Ammonium Solutions*
Amélioration de la sélectivité du captage du CO₂ dans les semi-clathrates hydratés en utilisant les ammoniums quaternaires comme promoteurs thermodynamiques
J.-M. Herri, A. Bouchemoua, M. Kwaterski, P. Brântuas, A. Galfré, B. Bouillot, J. Douzet, Y. Ouabbas and A. Cameira
- 969 > *Erratum*
J. E. Roberts

Enhanced Selectivity of the Separation of CO₂ from N₂ during Crystallization of Semi-Clathrates from Quaternary Ammonium Solutions

J.-M. Herri*, A. Bouchemoua, M. Kwaterski, P. Brântuas, A. Galfré, B. Bouillot, J. Douzet, Y. Ouabbas and A. Cameirao

Centre SPIN, Département PROPICE, UMR CNRS 5307, École Nationale Supérieure des Mines de Saint-Étienne, 158 Cours Fauriel, 42023 Saint-Étienne - France
e-mail: herri@emse.fr

* Corresponding author

Résumé — Amélioration de la sélectivité du captage du CO₂ dans les semi-clathrates hydrates en utilisant les ammoniums quaternaires comme promoteurs thermodynamiques — La réduction des émissions de CO₂ est très probablement l'un des enjeux importants de ce siècle. La capture puis le stockage géologique de ce gaz, à partir de sources industrielles ponctuelles et massives, est une voie d'importance. L'une des voies technologiques consiste à utiliser les clathrates hydrates, ou semi-clathrates hydrates, qui nécessitent de pressuriser le gaz en amont du procédé. Sous pression, l'eau et les gaz forment un solide qui encapsule préférentiellement le CO₂, puis le gaz peut-être ensuite récupéré sous pression après la dissociation du solide. L'abaissement de la pression opératoire est un objectif en soi afin de faire baisser les coûts opératoires. Cet abaissement peut être obtenu par l'utilisation de promoteurs thermodynamiques, dont les sels d'ammonium quaternaires constituent une famille intéressante puisqu'ils forment des solides naturellement anti-agglomérants, et plus facilement manipulables. Dans ce travail, nous présentons de nouveaux résultats expérimentaux sur les équilibres des semi-clathrates de (CO₂, N₂) en présence de Tetra-*n*-Butyl Ammonium Bromide (TBAB). Nous donnons des mesures expérimentales de pression et température en fonction de la concentration en TBAB. La pression opératoire peut être abaissée jusqu'à la pression atmosphérique. Nous donnons aussi une information supplémentaire portant sur la composition de l'hydrate. Nous observons que la sélectivité du CO₂ dans les semi-clathrates hydrates est bien meilleure que pour les clathrates hydrates traditionnels, sans promoteur thermodynamique.

Abstract — Enhanced Selectivity of the Separation of CO₂ from N₂ during Crystallization of Semi-Clathrates from Quaternary Ammonium Solutions — CO₂ mitigation is crucial environmental problem and a societal challenge for this century. CO₂ capture and sequestration is a route to solve a part of the problem, especially for the industries in which the gases to be treated are well localized. CO₂ capture by using hydrate is a process in which the cost of the separation is due to compression of gases to reach the gas hydrate formation conditions. Under pressure, the water and gas form a solid that encapsulates preferentially CO₂. The gas hydrate formation requires high pressures and low

temperatures, which explains the use of thermodynamic promoters to decrease the operative pressure. Quaternary ammoniums salts represent an interesting family of components because of their thermodynamic effect, but also because they can generate crystals that are easily handled. In this work, we have made experiments concerning the equilibrium of (CO_2, N_2) in presence of Tetra-*n*-Butyl Ammonium Bromide (TBAB) which forms a semi-clathrate hydrate. We propose equilibrium data (pressure, temperature) in presence of TBAB at different concentrations and we compare them to the literature. We have also measured the composition of the hydrate phase in equilibrium with the gas phase at different CO_2 concentrations. We observe that the selectivity of the separation is dramatically increased in comparison to the selectivity of the pure water gas clathrate hydrate. We observe also a benefice on the operative pressure which can be dropped down to the atmospheric pressure.

LIST OF SYMBOLS

A, B	A particular type of semiclathrate hydrate	ρ	(Mass) density, $[\rho] = \text{kg.m}^{-3}$
C	Langmuir constant of a guest molecule in a given cavity, $[C]$ depends on corresponding concentration/concentration dependent variable in relation to which it is defined, for example $[C_f] = \text{Pa}^{-1}$, whereas $[C_x]$ is dimensionless, or heat capacity $[C] = \text{J.K}^{-1}$	R	Universal gas constant, $R = (8.314472 \pm 0.000015) \text{ J.K}^{-1}.\text{mol}^{-1}$, or radius of a cavity, assumed to be of spherical geometry, $[R] = \text{nm}$
Δ	Finite difference between two values of a quantity	σ	Core distance at which attraction and repulsion between a guest host-pair balance each other, $[\sigma] = \text{pm}$
Δ_{α}^{β}	Finite difference between two values of a quantity for a process from a given initial state α to a final state β	T	Absolute temperature, $[T] = \text{K}$
EOS	Equation of State	TBAB	Tetra- <i>n</i> -Butyl Ammonium Bromide
f	Fugacity, $[f] = \text{Pa}$	θ	Fraction of sites occupied (by a particular species and for a specific type of cavity as indicated by additional subscripts), dimensionless
G	Growth rate, $[G] = \text{m.s}^{-1}$, or Gibbs energy, $[G] = \text{J}$	V	Volume, $[V] = \text{m}^3$
γ	Activity coefficient, dimensionless, or specific energy of surface $[\gamma] = \text{J.m}^{-2}$	w	Mass fraction (dimensionless)
k	Rate (kinetic) constant $[k] = \text{s}^{-1}$	x	Mole fraction of a chemical species, dimensionless; here mainly used to designate the mole fraction of guest species dissolved in the liquid phase in the immediate vicinity of the hydrate surface
k_B	Boltzmann's constant $k_B = (1.380\,648\,8 \pm 0.000\,001\,3) \times 10^{-23} \text{ J.K}^{-1}$	y	Mole fraction of a chemical species, dimensionless; here mainly used to designate the mole fraction of guest species in the gas phase
k_H^{∞}	Henry's constant at saturation pressure of the pure solvent, <i>i.e.</i> , at infinite dilution of the dissolved species, $[k_H^{\infty}] = \text{Pa}$	z	Mole fraction of a chemical species, dimensionless; here mainly used to designate the mole fraction of guest species in the cavities of the clathrate hydrate structure
M	Molar mass, $[M] = \text{g.mol}^{-1}$	Z	Compressibility factor
n	Amount of substance, <i>i.e.</i> mole number, $[n] = \text{mol}$		
R	Avogadro's number, $N_{Av} = (6.022\,141\,29 \pm 0.000\,000\,27) \times 10^{23} \text{ mol}^{-1}$		
ω	Intermolecular interaction potential, $[\omega] = \text{J}$		
v	Stoichiometric coefficient, or number of water molecules per number of guest molecules in a cage of of a given type I (hydration number), dimensionless		
P	Pressure, $[P] = \text{Pa}$		
r	Distance between the centre of the cavity and the guest molecule $[r] = \text{nm}$		

SUBSCRIPTS

A	Anionic species $A^{ z_A -}$
C	Cationic species $C^{z_C +}$
cell	Referring to the cell inside the experimental reactor
eq	Referring to a state of equilibrium
f	Indicating reference fugacity used as concentration dependent quantity

int	Interface between the integration layer and the diffusion layer
<i>i</i>	Index identifying a particular type of cavity
<i>j, j'</i>	Index characterising chemical species or chemical component (depending on the context), or guest specie
TBAB	Referring to Tetra- <i>n</i> -Butyl Ammonium Bromide
w	Water
<i>x</i>	Indicating the reference to the mole fraction as reference frame for the composition variable
R	Reactor
0	Indicating initial conditions for temperature and pressure

SUPERSCRIPTS

*	Indicating the unsymmetric convention for normalisation of activity coefficients, <i>i.e.</i> , the pure component reference frame for the solvent component and the infinitely dilution reference frame for the solute components and the solute species, respectively, or corresponding to the critical nuclei
⊖	Standard state; well defined state at reference conditions, where besides the state of aggregation or dilution, particularly the value for the pressure is fixed to its standard state value of 0.1 MPa. In this study used in the context of the standard value of the molality of $m^{\ominus} = 1 \text{ mol.kg}^{-1}$
○	Pure component state
∞	State of infinite dilution
G	Gas/vapour phase
H	Hydrate phase
L	Liquid phase
L _w	Liquid aqueous phase (depending on the context either an aqueous phase consisting of pure water) or a liquid mixed aqueous phase composed of an aqueous solution of a single binary electrolyte
ref	Reference state/frame in general
V	Vapour phase

INTRODUCTION

The CO₂ capture by using clathrates is a concept which takes profit of the physical interaction of gas molecules with water to be adsorbed selectively in a water-based solid structure being crystallized simultaneously, here

called gas hydrates, or clathrate hydrates, or semi-clathrates hydrates. The process consists in mixing water and the gas mixture containing CO₂ under hydrate-forming conditions of pressure and temperature. A thermodynamic promoter can be added in the system. It enters the hydrate structure and/or cavities to stabilize the hydrates. It enables the formation of hydrates at mild conditions of temperature and pressure and increases the selectivity of CO₂ in the hydrate phase.

The hydrate phase is made of clathrate hydrates and enclathred gas. According to the operative conditions of pressure and temperature, favored encapsulation of carbon dioxide in the hydrate phase is made while the other gases remain preferably in the gas, or liquid, phase. Pure carbon dioxide can then be recovered by the depressurisation and/or heating of the hydrate phase.

A concept of CO₂ capture by using clathrate hydrates has been patented by Dwain F. Spencer, firstly in 1997 and extended in 2000 (Spencer, 1997, 2000). This research (supported by the US Department of Energy) has been completed by additional works on the costing and design of single-stage or multi-stage processes for hydrate crystallisation. Deppe *et al.* (2002) have compared a hydrate-based technology for capturing CO₂ from CO₂/H₂ mixtures to conventional technologies (by amine and Selexol). The industrial context is a nominal 500 MW IGCC (Integrated Gasification Combined Cycle) coal gaseifier: the gas to be treated is the so-called syngas. The added capital cost for implementing the hydrate, amine and Selexol technologies is estimated to be respectively 23.9, 56.9 and 85.1 \$millions, and the operational cost is respectively 8, 21 and 14 \$/ton of CO₂. As a result, gas hydrate crystallization seems to offer the best economical potential.

An energy consumption estimation of a CO₂ separation from flue gases of natural gas-fired thermal power plant has also been made by Tajima *et al.* (2004). They showed that clathrate hydrate process consumes a considerable amount of energy, mainly due to the extremely high pressure conditions required for hydrate formation. By using thermodynamic additives, Duc *et al.* (2007) showed that the operative pressure can be reduced, improving the competitiveness of the process. They performed a complete sizing and costing for a hydrate-based treatment of flue gases (usually CO₂/CO/N₂ mixture) emitted by the steelmaking industry. The work has been done in the framework of the ULCOS European project during 6th EEC program (ULCOS, Ultra Low CO₂ emission for Steelmaking industry). The preliminary costing shows that the process is viable with a total cost (capital costing plus operative costing) of 22 € and 40 € per ton of captured CO₂, corresponding respectively to nitrogen free black furnace (with shaft

injection and plasma) and conventional black furnace (top gas and flue gas). The main part of the cost is due to compressors.

The concept of CO₂ capture by using hydrates implies the crystallization and the handling of slurries. From 15 years, the handling of high concentrated slurries has also questioned the community of refrigeration because of the application to thermal storage and transportation, by using Phase Change Materials (PCM). For example, PCM based on ice slurries has been developed by several industries because of their potential in refrigeration (negative temperature). To that aim, the fluid is composed of water that can crystallize to form ice and the melting point is adjusted by adding appropriate additives, such as alcohols. Different kinds of ice slurry generators have been developed (Meunier *et al.*, 2007). The more accessible technology is the scraped surface heat exchanger patented by Sunwell system (Gibert, 2006) or the Heatcraft generator patente by Lennox company (Compingt *et al.*, 2009).

However, for applications above 273.15 K, *i.e.* air conditioning systems, the use of ice slurry is no longer applicable because the ice melting point cannot be adjusted to positive temperature. Several authors (Lipkowski *et al.*, 2002; Obata *et al.*, 2003; Oyama *et al.*, 2005) have shown that some kind of quaternary ammonium can be used as PCM for air conditioning applications. For example, Tetra-Butyl Ammonium Bromide (TBAB) forms hydrate slurries very similar to ice slurries, but with a melting point that can be adjusted from 273.15 K to 285.15 K depending on the TBAB concentration (Fig. 1). A previous study has demonstrated the possibility to handle such suspensions (Darbouret, 2005) up to solid concentration of 30% vol.

The JFE Engineering Corporation has designed and commercialized a technology which uses TBAB hydrates slurry also (Takao *et al.*, 2001, 2002, 2004; Mizukami, 2010; Ogoshi *et al.*, 2010). Their first prototype was built in 2005 and today, approximately 10 systems have been sold and have shown the feasibility of this process to cooling power up of 2 MW. In general, this company transforms an old system of air conditioning which is using cold water. Water circulating in the secondary loop is replaced by a TBAB slurry.

So, there is a clear convergence on the technologies that can be used to capture CO₂, or to store energy. For low scale applications (air conditioning), the technology begins to be mature. However, for CO₂ capture, at a bigger scale, there is no prototype to validate the concept. Only laboratory pilot scale units exist: bubble reactors for CO₂/N₂ separation (Douzet *et al.*, 2011, 2013) or CO₂/H₂; (Xu *et al.*, 2012), combination of a bubble and stirred reactor (Linga *et al.*, 2010), or spray reactor (Brinchi *et al.*, 2011) for CO₂/CH₄ separation.

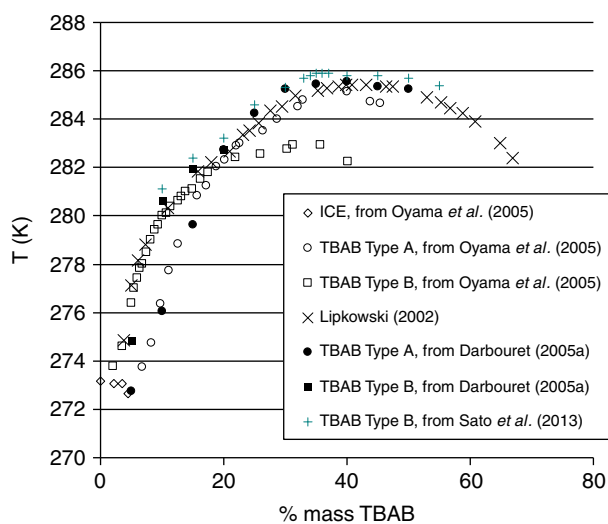


Figure 1

T,x- phase diagram of TBAB-water binary system in the region of crystallization of clathrates polyhydrates (Oyama *et al.*, 2005; Lipkowski *et al.*, 2002; Darbouret, 2005).

Also, and because the operative cost is mainly driven by the operative pressure, studies are carrying on to understand the benefices of additives which can deplete the pressure (thermodynamic promoters) and/or orientate the selectivity (kinetic promoters).

1 STATE OF THE ART

The clathrates hydrates, and semi-clathrate hydrates, are ice-like compounds in the sense that they correspond to a re-organisation of the water molecules to form a solid. The crystallographic structure is based on H-bonds. The clathrates of water are also designated improperly as “porous ice” because the water molecules build a solid network of cavities in which gases, volatile liquids or other small molecules could be captured.

The clathrates hydrates of gases, called gas hydrates, have been studied intensively due to their occurrence in deep sea pipelines where they cause serious problems of flow assurance.

Each structure is a combination of different types of polyhedra sharing faces between them. Jeffrey (1984) suggested the nomenclature e^f to describe each polyhedra: e is the number of edges of the face, and f is the number of faces with e edges.

The clathrates of gas can be stabilized by thermodynamic promoters. Two classes of thermodynamic promoters can be distinguished. The first ones are species

which are enclathred in the cavities without modifying the structure of the hydrates. This kind of hydrate is still called clathrate hydrate and its structure belongs to the classical sI, sII or sH structure. The second class of thermodynamic promoters modifies the structure. The new structure is called semi-clathrate hydrates.

2 CLATHRATE HYDRATES

The classical sI, sII or sH structure (Tab. 1) can be stabilized by the presence of promoters. Two promoters, tetrahydrofuran and cyclopentane, have been well described in the literature for their remarkable properties to drop the operative pressure to form gas hydrates.

2.1 Tetrahydrofuran: An Example of Water Soluble Additive

TetraHydroFuran (THF) forms structure II hydrates in which THF occupies the large cavity $5^{12}6^4$ and gas competes with THF for the occupation of the large cavity and/or occupies the small cavity. THF is a water-soluble additive. With water, they are completely miscible in the liquid state over the whole composition range in the pressure and temperature domain of hydrate formation (Riesco and Trusler, 2005). The equilibrium pressure reduction effect to form hydrates is dependent on the relative concentration of THF. It is important to notice that in presence of pressurized carbon dioxide (temperature above 290 K and a pressure above 2.0 MPa), Sabil et al. (2010) observed that water and THF phase split in two liquids phases (in presence of a solution of 5% mole of THF in water). Over the years, many authors reported hydrate dissociation data of the system

{THF + water + gas}. Only works where nitrogen and carbon dioxide were used are presented in the following paragraph and summed up in Table 2.

2.1.1 Benefits of THF on the Equilibrium of Pure Gases

Seo et al. (2001, 2008) studied the hydrate dissociation pressure – temperature data {H₂O + THF + pure gas (CO₂ or N₂)} for several compositions of THF (1 to 5%mol of THF in water) and the hydrate dissociation pressure – temperature data {H₂O + THF + CH₄} for 3%mol of THF.

Firstly, their studies focused on showing the stabilization effect of THF on hydrate formation compared to the effect of others water miscible promoters (propylene oxide, 1,4-dioxane, acetone). For a concentration of promoter of 3%mol, THF was found to be the most interesting for each gas (CO₂, N₂ and CH₄).

Secondly, the effect of THF concentration from 1 to 5%mol on the equilibrium hydrate dissociation pressure-temperature data has been studied. The pressure decreased rapidly up to 1%mol of THF, but very slowly above 1%mol for each case study (CO₂ and N₂).

Delahaye et al. (2006) also investigated the hydrate dissociation pressure – temperature data {H₂O + THF + CO₂} for THF concentration in the range of 1.6 to 3.0%mol, and the latent heat of dissociation of the mixed hydrates (CO₂/THF/water). Like Seo et al. (2008), the authors observed the drastic reduction of the hydrate pressure formation with a few mole of THF in the system.

Sabil et al. (2010) also examined the complete hydrates dissociation lines for the system {H₂O + THF + CO₂} at a THF concentration of 5%mol for different carbon dioxide concentrations.

TABLE 1
Structure of gas hydrates (Sloan and Koh, 2008)

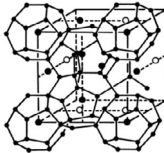
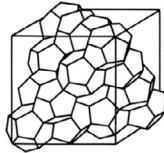
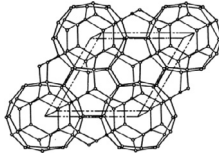
	SI		SII		SH		
							
Cavity (*)	5 ¹²	5 ¹² 6 ²	5 ¹²	5 ¹² 6 ⁴	5 ¹²	4 ³ 5 ⁶ 6 ³	5 ¹² 6 ⁸
Type of cavity	1	2	1	3	1	5	4
Number of cavity	2	6	16	8	3	2	1
Average cavity radius (nm)	0.395	0.433	0.391	0.473	0.391	0.406	0.571
Variation in radius (%)	3.4	14.4	5.5	1.73			

TABLE 2
Experimental studies on gas hydrate in presence of tetrahydrofuran

Authors	Gas(es)	Promoters	Pressure and temperature area
Seo <i>et al.</i> (2001)	N ₂ , CH ₄	THF (3%mol) > acetone (3%mol) > 1,4-dioxane (3%mol) > propylene oxide (3%mol) THF (5%mol) > THF (3%mol) > THF (1%mol)	For N ₂ /THF/water system: $T = [280.85-293.75]$ K $P = [3.12-10.872]$ MPa For CH ₄ /THF (3%mol)/water system: $T = [292.16-302.46]$ K $P = [2.02-8.91]$ MPa
Delahaye <i>et al.</i> (2006)	CO ₂	THF (1.6-3%mol)	$P = [0.2-3.5]$ MPa $T = [286-291]$ K
Seo <i>et al.</i> (2008)	CO ₂	THF (3%mol) > propylene oxide (3%mol) > > 1,4 dioxane THF (5%mol) > THF (3%mol) > THF (1%mol)	For CO ₂ /THF/water system: $T = [270-290]$ K $P = [0.2-4.7]$ MPa
Sabil <i>et al.</i> (2010)	CO ₂	THF (5%mol)	For CO ₂ /water system: $T = [275.12-290]$ K $P = [1.51-5.28]$ MPa For CO ₂ /THF/water system and depending on CO ₂ concentration: $T = [285.39-301.46]$ K $P = [0.9-7.05]$ MPa
Yang <i>et al.</i> (2011)	N ₂ , O ₂ , air	THF (5-5.13%mol)	For N ₂ /THF/water system: $T = [295.75 -303.60]$ K $P = [10.95- 29.527]$ MPa For O ₂ /THF/water system: $T = [286.10 -303.63]$ K $P = [2.130-25.812]$ MPa For air/THF/water system: $T = [281.84 -299.41]$ K $P = [0.981-16.685]$ MPa
Kang and Lee (2000) Kang <i>et al.</i> (2001)	CO ₂ /N ₂	THF (1, 3%mol)	For CO ₂ /N ₂ /water system: $T = [274, 277, 280]$ K $P = [1.394-32.308]$ MPa For CO ₂ /N ₂ /THF/water system: $T = [274.85-295.45]$ K $P = [0.2-12.905]$ MPa
Linga <i>et al.</i> (2007a,b)	(16.9%/83.1%) CO ₂ /N ₂	THF (1%mol)	For CO ₂ /N ₂ /water system (y_{CO_2} , initial mole fraction = 0.169): $T = 273.7$ K $P = [9, 10, 11]$ MPa For CO ₂ /N ₂ /THF/water system: $T = 273.7$ K $P = 1.5$ MPa
Linga <i>et al.</i> (2010)	(16.9%/83.1%) CO ₂ /N ₂	THF (1%mol)	$P = [1.5, 2.3, 2.5]$ MPa $T = 273.7$ K
Herslund <i>et al.</i> (2013)	CO ₂ /N ₂	THF 5%mol	$T = 283.3$ to 285.5 K

The authors discovered a four-phase equilibrium region with three fluid phases at temperatures above 290 K and pressures above 2.0 MPa: a water-rich

with a constant amount of carbon dioxide, a carbon dioxide in an organic-rich, the vapor phase and the hydrate phase.

Finally, Yang *et al.* (2011) studied the hydrate dissociation pressure – temperature data {H₂O + THF + pure gas (N₂)} for THF concentration of 5%mol. The authors also provided equilibrium phase hydrate data for {O₂ + THF + water}, {air + THF + water}. Their research focused on finding valuable information on the air separation by hydrate crystallization.

2.1.2 Benefits of THF on Gas Mixtures

Recovering CO₂ from a gas mixture of CO₂/N₂ in presence of THF was the purpose of the works of (Kang and Lee, 2000; Kang *et al.*, 2001; Linga *et al.*, 2007a,b). The authors measured the hydrate dissociation data for several mixtures of CO₂ and N₂ without any promoter and in presence of THF. As for pure gases, with aqueous solutions containing 1 and 3%mol of THF, a drastic drop of equilibrium dissociation pressure has been observed from the moment the THF concentration reached 1 mole percent (Kang and Lee, 2000; Kang *et al.*, 2001). Moreover, a benefit of THF is observed on the selectivity of the separation. Pressure-composition diagrams of the {H₂O + THF + CO₂/N₂} system for 1 mole percent of THF and the {H₂O + CO₂/N₂} system have been drawn at three temperatures (Tab. 2) for several compositions of the gas mixture CO₂/N₂. The respective hydrate compositions of the mixed hydrates with and without THF have been added on the diagrams. Kang and Lee (2000) showed that the CO₂ selectivity in the mixed hydrate phase has been lowered in the mixed hydrate when the THF has been used as a hydrate promoter.

Linga *et al.* (2007a,b) tested a THF concentration of 1%mol and studied the gas uptake and the rate of the crystallization. THF reduced the induction time but also the growth rate of the crystallization.

The authors did not estimate the carbon dioxide selectivity and did not calculate the gas storage capacity.

Finally, Linga *et al.* (2010) investigated the formation of gas hydrate with one composition of gas mixture at THF concentrations of 1 and 1.5%mol. The authors estimated the gas uptake and the CO₂ recovery and compared them to the results reported in the literature with Tetra-*n*-Butyl Ammonium Bromide and Tetra-*n*-Butyl Ammonium Fluoride (Fan *et al.*, 2001; Li S. *et al.*, 2009).

2.2 Cyclopentane: An Immiscible Organic Additive

Cyclopentane (CP) is described in the literature as an excellent thermodynamic promoter. It forms structure II hydrate without any gas (Nakajima *et al.*, 2008) but competes with CO₂ to occupy the large cavity 5¹²6⁴. Cyclopentane is a hydrophobic compound and needs

to be dispersed in water. So, the main difference with THF is the low solubility of CP in water.

Fan *et al.* (2001) were the first to report the quadruple equilibrium point (CP hydrate-liquid water-organic liquid-vapor) at a temperature of 280.22 K and a pressure of 0.0198 MPa (abs).

As for THF, many authors reported the hydrate dissociation data of the system (THF + water + pure CO₂, pure N₂, or CO₂ + N₂): their works are summed up in Table 3 and detailed in the following paragraph.

Zhang and Lee (2009a) and Zhang *et al.* (2009) determined hydrate dissociation data for {H₂O + (CO₂ + CP)} system. Dissociation conditions for {H₂O + (CO₂ + CP)} hydrate have been compared with the dissociation data for {H₂O + (CO₂ + TBAB)} with a TBAB weight fraction of 0.427 (Arjmandi *et al.*, 2007) and for {H₂O + (CO₂ + THF)} with a THF molar fraction of 3 percent (Delahaye *et al.*, 2006). CP appears to be a better additive than TBAB to decrease the equilibrium pressure.

Zhang and Lee (2009b) also studied the potential of using CP as a kinetic promoter in a static autoclave at a low temperature.

Mohammadi and Richon (2010) compared the stabilization effect of CP on hydrate formation of {H₂O + (CO₂ + CP)} gas hydrate to the effect of several organic promoters (example: methyl-cyclopentane, methyl-cyclohexane, and cyclohexane). For volume fraction of promoter of 10% in water, among the promoters, CP promotion effect was the highest. Experimental dissociation data for clathrate hydrates of cyclopentane and carbon dioxide have been also reported. Data were in good agreement with the study of Zhang and Lee (2009a) and Zhang *et al.* (2009).

Experimental hydrate dissociation data for {H₂O + (N₂ + CP)} system were first published by Tohidi *et al.* (1997). They tested the potential of using cyclopentane to decrease the equilibrium pressure when gas hydrates of nitrogen and promoter (cyclopentane or neopentane) are formed. CP promotion effect has also been compared in that case to several organic promoters of the literature (cyclohexane and benzene). It was found to be the strongest promoter, just above neopentane.

Mohammadi and Richon (2011) and Du *et al.* (2010) completed the experimental hydrate dissociation data for {H₂O + (N₂ + CP)} system and their results were in good agreement.

For CO₂/N₂ gas mixture, Li S. *et al.* (2010) preliminary showed that gas hydrates could be enriched in CO₂ in presence of cyclopentane. The authors studied two different situations: CP dispersed in an emulsion or a buoyant CP phase on the top of the liquid water phase. Differences in the separation efficiency have been

TABLE 3
Experimental studies on gas hydrate in presence of cyclopentane

Authors	Gas(es)	Promoters	Pressure and temperature area
Tohidi <i>et al.</i> (1997)	N ₂	Promoter volume fraction: no indicated Cyclopentane > neopentane > cyclohexane > benzene	For N ₂ /CP/water system: T = [282.9 -289.1] K P = [0.641-3.496] MPa
Mohammadi and Richon (2009, 2010, 2011)	CO ₂ , N ₂	For CO ₂ (promoter volume fraction in water: 10%): Cyclopentane >> cyclohexane > methylcyclohexane, isopentane, methylcyclopentane Cycloheptane, cyclooctane = no promotion effect For N ₂ (promoter volume fraction in water: 10%): Cyclopentane >> cyclohexane > methylcyclohexane = methylcyclopentane	For CO ₂ /CP/water system: T = [284.3-291.8] K P = [1.82-2.52] MPa For N ₂ /CP/water system: T = [281.7-290.2] MPa P = [0.25-4.06] MPa
Zhang and Lee (2009a) Zhang <i>et al.</i> (2009)	CO ₂	Cyclopentane (1-60%vol. in water)	P = [0.89-3.51] MPa T = [286.65-292.61] K
Zhang and Lee (2009)	CO ₂	Cyclopentane (1-10%vol. in water)	P = [1.90-3.42] MPa T = [273.41-273.76] K
Du <i>et al.</i> (2010)	N ₂	Cyclopentane (30.5%vol. in water)	P = [2.27-30.40] MPa T = [281.3-303.1] K
Li S. <i>et al.</i> (2010)	(16.6%/83.4%) CO ₂ /N ₂	Cyclopentane (20% weight fraction of water)	P = [2.49-3.95] MPa T = 281.25 K
Herslund <i>et al.</i> (2013)	CO ₂ /N ₂	Cyclopentane	T = [275.25-285.2] K

reported. This difference implies that the authors have not reached the thermodynamic equilibrium in their work. In fact, we will comment this point in our discussion, but it appears that the formed hydrate from a gas mixture are not at equilibrium, and that its composition is directly dependent on kinetic considerations, and so is indirectly dependent on the geometry of the system.

3 SEMI-CLATHRATE HYDRATES

Another class of clathrates, called semi-clathrates, can be formed in presence of electrolytes, such as alkyls Ammonium salts (this work) or alkyls Phosphonium salts (Sato *et al.*, 2013). It forms, in presence of water, and without any gas, a semi-clathrates hydrate crystal, even at atmospheric pressure (McMullan and Jeffrey, 1959). They are qualified as peralkylonium polyhydrates and have been the research project of the Russian team of Dyadin *et al.* over decades and were only published in english in 1984, 1985 and 1995 (Dyadin and Udachin, 1984, 1987; Dyadin *et al.* 1995). In contrast to gas hydrates, the cation is the guest situated in the frame-

work cavities and separated from the host- molecules by the distance not less than the sum of the van der Waals radii (hydrophobic inclusion). “A simple anion of a halogenide type displaces the water molecule in the framework, forming H-bonds together with the neighbouring molecules (hydrophilic inclusion), causing the framework to become of water-anion type. The anion with a hydrophobic part includes in a hydrophilic way with the polar group, forming the framework knot or edge, the hydrocarbon part being situated in one of the framework cages” (Dyadin and Udachin, 1984).

So, they are called semi-clathrates due to the fact that the crystalline water network is broken in order to incorporate the cation of the compound. For instance, in the case of TBAB hydrate, the nitrogen atom at the center of the four butyl radicals takes the place of a water molecule effectively, “breaking” the four surrounding cages and creating a larger cavity made from smaller ones. Therefore the hydration number will change regarding gas hydrates because less water molecules in a similar structure, due to their replacement by the cation of the semi-clathrate, will be present. Bromide atoms and water molecules form

TABLE 4
Anions of semi-clathrates (Dyadin and Udachin, 1987; Dyadin et al., 1995)

Anion	Examples
Halogens	Cl ⁻ , Br ⁻
Hydroxide	OH ⁻
Carboxylates	HCO ₂ ⁻ , C ₃ H ₇ CO ₂ ⁻
Branched carboxylates	iso-C ₃ H ₇ CO ₂ ⁻ , meta-ClC ₄ H ₄ CO ₂ ⁻
Linear dicarboxylates	CH ₂ (CO ₂ ⁻) ₂ , (CH ₂) ₃ (CO ₂ ⁻) ₂
Branched dicarboxylates	iso-C ₃ H ₇ (CO ₂ ⁻) ₂
Aromatic dicarboxylates	o-C ₆ H ₄ C ₂ O ₄ ²⁻
Oxalates	C ₂ O ₄ ²⁻ , (CH ₂) ₃ C ₂ O ₄ ²⁻
Oxides	O ⁻
Phosphates	HPO ₄ ²⁻ , PO ₄ ³⁻
Chromates	CrO ₄ ²⁻
Nitrates	NO ₃ ⁻
Bicarbonates	HCO ₃ ⁻ , CO ₃ ²⁻
Chlorates	ClO ₃ ⁻
Alkane sulfonates	HSO ₃ ⁻
Tungstates	WO ₄ ²⁻

the cage structure. Tetra-*n*-Butyl Ammonium is located at the centre of four cages (Shimada *et al.*, 2005b) and the butyl groups occupy the cavities. There is a large number of semi-clathrate compounds due to the different cation and anion they possess. Tables 4 and 5 shows the anions and cations that can be found in a semiclathrate. Furthermore, it is possible that some semi-clathrates have different cations.

With a wide range of anions and cations that can compose a semi-clathrate, it is not a surprise that many different crystalline structures can be formed. A detailed review has been made by Dyadin and Udachin in 1987 which continues to be the reference on the subject (Dyadin and Udachin, 1987).

TBAB has been extensively studied in reason of a direct application for air conditioning as a phase change material (Lipkowski *et al.*, 2002; Oyama *et al.*, 2005; Kamata *et al.*, 2004; Darbouret *et al.*, 2005; Lin *et al.*, 2008; Arjmandi *et al.*, 2007; Li S. *et al.*, 2009). Tetra butyl ammonium bromide salt forms at least four different structures with hydration number of 24, 26, 32 and 36 (Lipkowski *et al.*, 2002). Only one of the crystallographic

TABLE 5
Cations of semi-clathrates (Dyadin and Udachin, 1987; Dyadin et al., 1995)

Cation	Examples
Linear alkyls ammoniums	(C ₄ H ₉) ₄ N ⁺ , (C ₃ H ₇) ₄ N ⁺
Branched alkyl ammoniums	(iso-Am) ₄ N ⁺
Linear alkyl phosphoniums	(C ₄ H ₉) ₄ P ⁺
Branched alkyl ammoniums	(iso-Am) ₄ P ⁺
Linear alkyl phosphines	(C ₄ H ₉) ₃ P ⁺
Linear alkyl ternary ammoniums	(C ₄ H ₉) ₃ N ⁺
Linear alkyls arsines	(C ₄ H ₉) ₃ As ⁺
Linear amine phosphoniums	(C ₄ H ₉) ₃ (C ₃ H ₅ NCH ₂)P ⁺
Linear alkyl diammoniums	(CH ₂)[(C ₄ H ₉) ₄ N] ²⁺

structures of semi-clathrate hydrates has been determined precisely by McMullan and Jeffrey (1959) and completed by Shimada (2005b).

Oyama *et al.* (2005) reported some thermal properties of TBAB semi-clathrates. They determined the phase diagram of semi-clathrates hydrates under the conditions of atmospheric pressure, and also measured latent and specific heats capacity. From the phase diagram, the congruent melting points of two different TBAB semi-clathrates structures were determined (285.15 K and 282.55 K for semi-clathrates with respectively a hydration numbers of 26 and 38). It is interesting to notice that Dyadin *et al.* (1995) did not find the structure with 38 as hydration number. It shows again that semiclathrate formation is a difficult process to predict. Figure 1 plots the data of Oyama *et al.* (2005) competed with some data from literature. A complete reviewing off all the equilibrium data can be in Sato *et al.* (2013).

Davidson (1973) suggested that these semi-clathrates crystals do not encage gas molecules, but Shimada *et al.* (2005a) and Duc *et al.* (2007) have given opposite results or opinions. Shimada *et al.* (2003, 2005a) has supposed that TBAB semi-clathrates could encage small gas molecules. In fact, based on the structure analyze of pure TBAB semi-clathrates (formula (n-C₄H₉)₄N⁺Br, 38H₂O), they supposed that the structure could encapsulate the gas in the free cavities (Fig. 2). Duc *et al.* (2007) have experimentally confirmed that semi-clathrates can encapsulate up to 40 M³ STP of gas per cubic meter of solid.

Since this period, a huge quantity of experimental results has been produced which gives evidence of the

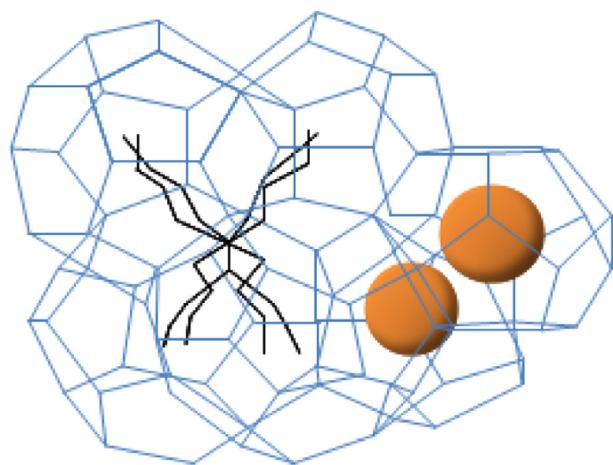


Figure 2
Structure of gas TBAB semi-clathrates (Shimada *et al.*, 2005b).

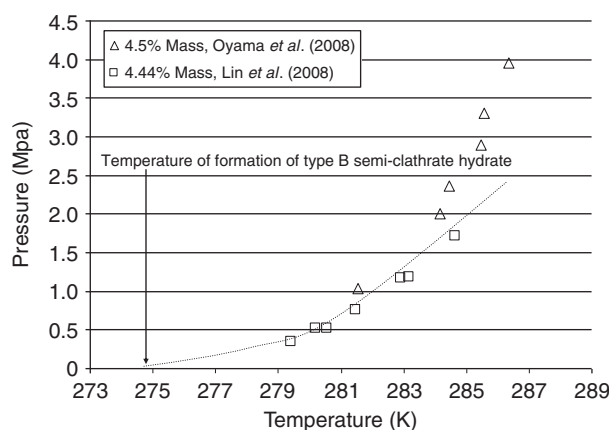


Figure 3
CO₂-TBAB semi-clathrate equilibrium curve at TBAB mass fraction of 4.44-4.5%, from Oyama *et al.* (2008) and Lin *et al.* (2008).

enclathration of gases in the TBAB structure. The question that remains is which structure is formed. In fact, facing the variety of possibilities, and except the work of Shimada *et al.* (2005b) who clearly identified one structure in presence of gas, we do not have evidence of the crystallographic structure formed.

3.1 (Pressure-Temperature) Equilibrium with TBAB, CO₂ and N₂

In the recent years, many experimental data have been produced about the equilibrium of TBAB semi-clathrate in presence of pure CO₂ and pure N₂ gas. Also, a model has been produced by Paricaud (2011) to predict the pressure and temperature of equilibrium as a function of the TBAB mass fraction for only one type of hydrate structure. This model will not be described in detail in this publication, but some of its fundamental equations will be used to explain the observations of the experimental results.

Arjmandi *et al.* (2007) have given CO₂-TBAB semi-clathrate equilibrium data at TBAB mass fraction of 0.1 and 0.4. Duc *et al.* (2007) have determined few points at TBAB mass fraction of 0.05, 0.09, 0.5 and 0.65. Lin *et al.* (2008) did a complete study for TBAB mass fraction of 0.044, 0.07 and 0.05. Oyama *et al.* (2008) gave equilibrium data of CO₂ semi-clathrate at TBAB mass fraction of 0.1. But also, they produced data at very low mass fraction of 0.01, 0.02, 0.03 and 0.045 without formation of the semi-clathrate hydrate but only formation of the clathrate hydrate. Lastly, Deschamps and

Dalmazzone (2009) have given few points at TBAB mass fraction of 0.4.

Experiments about N₂-TBAB semi-clathrate equilibrium are less numerous. Arjmandi *et al.* (2007) have given N₂-TBAB semi-clathrate equilibrium data at TBAB mass fraction of 0.1. Duc *et al.* (2007) have determined few points at TBAB mass fraction of 0.05, 0.09, 0.5 and 0.65. Deschamps and Dalmazzone (2009) have given few points at TBAB mass fraction of 0.4.

Figures 3, 4 and 5 show some of the experimental data for CO₂-TBAB semi-clathrate. All the data are not coherent. In Figure 3, for two similar TBAB mass fractions, we can distinguish two different equilibrium curves (Oyama *et al.* in 2008, and Lin *et al.* in 2008). At TBAB mass fraction of 9-10 percent (Fig. 4), the equilibrium data of Arjmandi *et al.* (2007), Duc *et al.* (2007), Oyama *et al.* (2008) and Lin *et al.* (2008) do not seem in coherence together. But, at TBAB mass fraction of 0.4 (Fig. 5), the data from Arjmandi *et al.* (2007), Duc *et al.* (2007) and Deschamps and Dalmazzone (2009) appear to be coherent together. The difference between the authors can be explained by the difficulty to crystallize the same structure. In fact, as we underlined before, the TBAB semi-clathrate can crystallize under 4 structures, and at least two of them can capture gas (Paricaud, 2011).

Independently of the difference between the experiments, it can be stated that the equilibrium pressure decreases as the temperature decreases. The different authors reported equilibrium pressure down to 0.5 MPa, but never close to the atmospheric pressure.

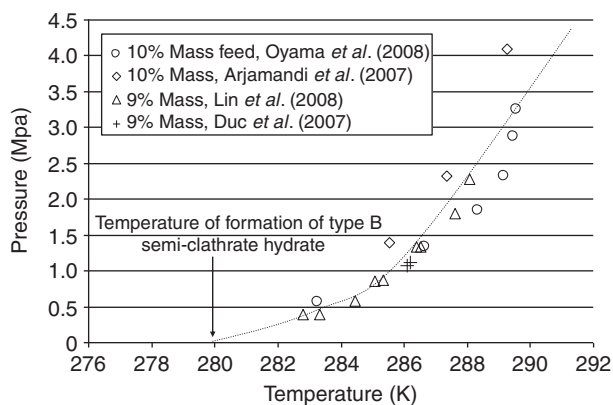


Figure 4

CO₂-TBAB semi-clathrate equilibrium curve at TBAB mass fraction of 9-10 percent, from Arjamandi *et al.* (2007), Duc *et al.* (2007), Oyama *et al.* (2008) and Lin *et al.* (2008).

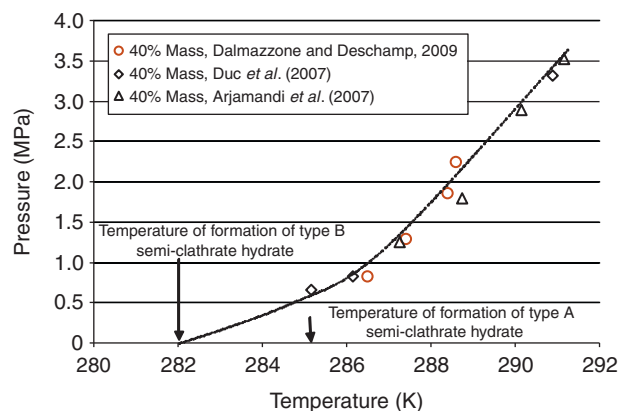


Figure 5

CO₂-TBAB semi-clathrate equilibrium curve at TBAB mass fraction of 40 percent, from Arjamandi *et al.* (2007), Duc *et al.* (2007), Deschamps and Dalmazzone (2009).

In fact, at low pressure, the kinetics slow down and the crystallization time becomes too long to be observed. But, from a theoretical point of view, we will demonstrate that the equilibrium pressure tends to 0 as the temperature tends to the temperature of equilibrium of the pure TBAB clathrate hydrate.

For example, at TBAB mass fraction of 4.5 percent, Figure 1 shows that type B semi-clathrate hydrate is stable at temperature down to 274-275 K. In Figure 3, this temperature can be understood as the limit temperature at which the extrapolated equilibrium pressure becomes zero. At TBAB mass fraction of 10 percent, Figure 1 shows that pure type A semi-clathrate hydrate (without gas) is stable at temperature down to 276-277 K, and that pure type B semi-clathrate hydrate (without gas) is stable at temperature down to 279.5-280.5 K. In Figure 4, we can observe that the temperature of 280 K is the limit temperature at which the extrapolated equilibrium pressure becomes zero. The same analysis can be done in Figure 5 by considering that the Type B still continues to be the crystallized structure in solution at TBAB mass fraction of 0.4. From Figure 1, we can observe that pure type A semi-clathrate hydrate (without gas) is stable at a temperature down to 285 K, and that pure type B semi-clathrate hydrate (without gas) is stable at a temperature down to 280 K. Figure 5 shows that the value of 280 K seems to be the limit temperature at which the extrapolated equilibrium pressure becomes zero.

Remark: Mixed promoter systems can also be an alternative system to enhance the carbon dioxide selectivity

and to drastically decrease the operative pressure. In presence of carbon dioxide/hydrogen (38.6/61.4 mole percent mixture), Li X.-S. *et al.* (2011, 2012) tested hydrate formation with the simultaneous presence of TBAB and cyclopentane. They compared the gas uptake, the CO₂ selectivity in the hydrate phase to the single promoter systems ({CP + gas + water} and {TBAB + gas + water}). The system with the CP/TBAB solution volume ratio of 5 percent and a concentration of 0.29 mole percent of TBAB was the optimum to obtain the largest gas uptake and the highest CO₂ selectivity at 274.65 K and 4.0 MPa. The selectivity of CO₂ over hydrogen was 91.6 mole percent in the mixed hydrate phase when the carbon dioxide concentration in the residual gas was 13.5 mole percent. In comparison, in presence of the TBAB/(CO₂ + H₂)/water system, the selectivity of CO₂ was 93.6 mole percent when the carbon dioxide concentration in the residual gas was 18 mole percent in the same conditions of temperature and pressure. The authors observed that a synergistic effect may occur: cyclopentane does not only form sII hydrates but also takes part in the semi-clathrate hydrate structure (Li X.-S. *et al.*, 2012).

4 EXPERIMENTAL SET-UP

An experimental apparatus (Fig. 6) has been built to investigate the gas hydrates formation and dissociation with and without the presence of TBAB. The

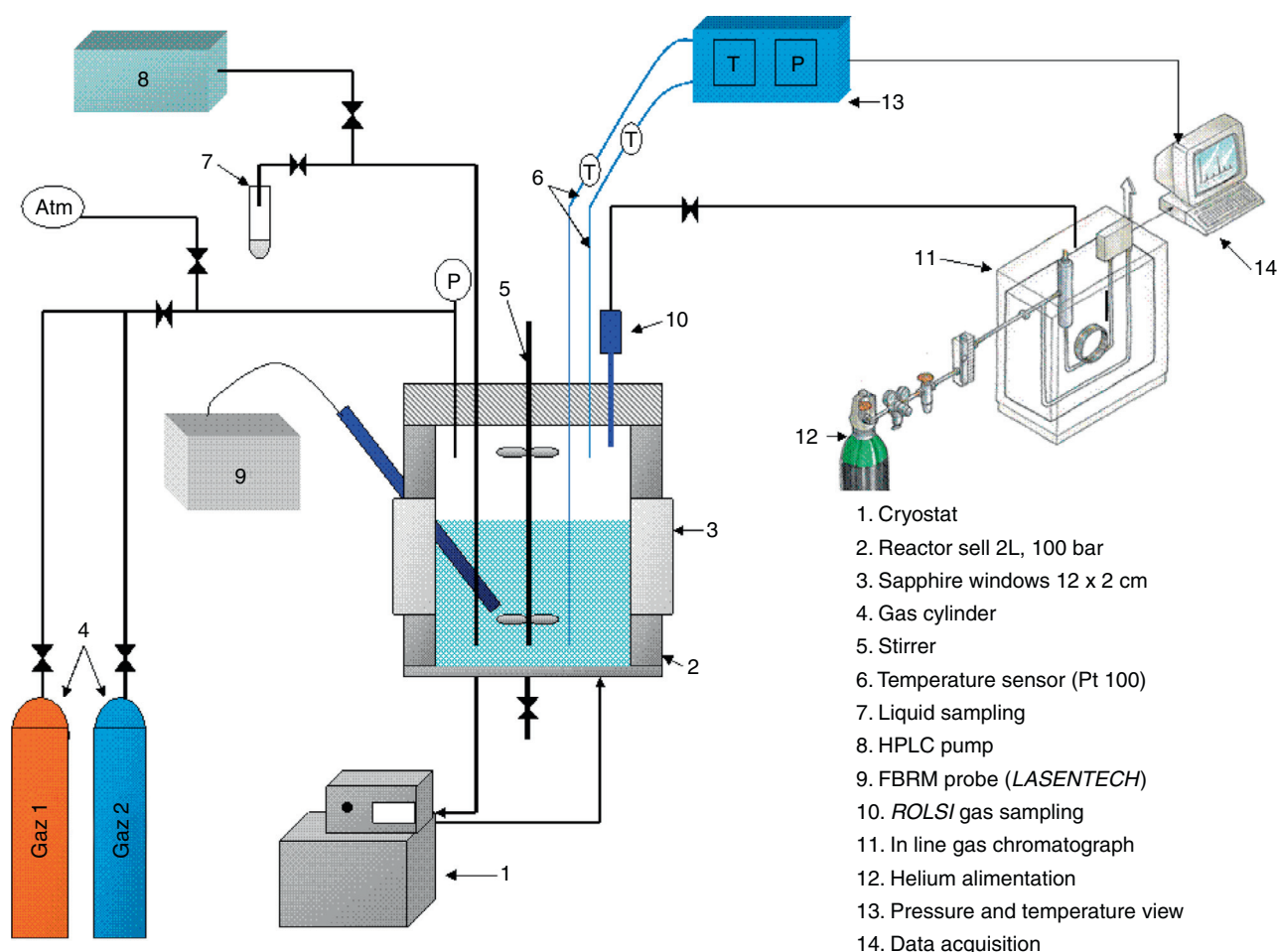


Figure 6
 Experimental set-up.

thermodynamic equilibrium conditions have been obtained by determining the pressure, the temperature and the compositions of all gas, liquid and hydrate phases. The experimental set-up is a stainless steel high pressure batch reactor (autoclave) with a measured volume of $V_R = 2.51 \pm 0.03 \text{ dm}^3$. It is surrounded with a double jacket connected to an external cooler (Huber CC-505) with a controller CC3 of 0.02 K precision. Two polycarbonate windows ($12 \times 2 \text{ cm}$) are mounted on both sides of the reactor, allowing the visual observation of the hydrates. A Pyrex cell of volume V_{cell} is located in the stainless steel autoclave in which the pressure can be raised up to 10 MPa. The Pyrex cylinder is filled with a volume of $V_{liq,0} = 1 \text{ dm}^3$ of water containing TBAB at concentration between 5 wt% and 40 wt%. The liquid is injected in the pressurized reactor by using a HPLC (High Performance Liquid Chromatography)

pump (JASCO-PU-1587). The initial gas mixture is prepared by injecting each of the two gases directly into the reactor and is performed separately in two successive steps by means of two different valves. The composition of the gas phase is determined on-line by using a gas chromatograph, after sampling, by a ROLSI instrument. This device collects a small gas sample of a defined volume, which is then directly injected into the loop of the gas chromatograph. The volume of the sample is in between $1 \mu\text{m}^3$ and $5 \mu\text{m}^3$ and is considered as negligibly small relative to the total volume of the gas phase in the reactor which is of the order of magnitude of 1.5 dm^3 .

A four vertical-blade turbine impeller ensures stirring of the suspension during crystallization. Temperature is monitored by two Pt100 probes in the bulk and the gas phases. Pressure is measured by means of a pressure transducer (range: 0-10 MPa) with a precision of

±0.05 MPa. The data acquisition unit (P , T) is connected to a personal computer.

A classical valve is used to take a sample of 1 cm³ of liquid. It is analyzed by refractometry to determine the TBAB concentration. The sample is also analysed in a DIONEX ionic exchange chromatograph (off-line) to measure the concentration of the electrolyte tracer LiNO₃ (see experimental procedure for details, Herri et al., 2011).

5 EXPERIMENTAL PROCEDURE

The hydrate is obtained by crystallization of pure gases (CO₂, N₂) or gas mixture with a liquid phase containing water and the salt.

At the beginning, the reactor is closed and vacuumed with a vacuum pump. Then, the cell is flushed three times with the gas to be studied. It erases any trace of other gases used in a previous experiment. Then, the reactor is vacuumed again.

After, the reactor is pressurized with the pure gas (CO₂ or N₂) at initial pressure P_0 . The gas phase is sampled with the ROLSI instrument and on-line analysed by gas chromatography to check the gas purity. The gas phase is stirred, cooled down, and maintained at the operative temperature (here called T_0 , typically in the temperature range of 278 to 286 K).

When a gas mixture of CO₂/N₂ is studied, the following experimental procedure is used. The reactor is pressurised with the first gas (CO₂ or N₂) to the desired pressure and analysed by gas chromatography to check the gas purity. After stabilisation of temperature and pressure, the second gas is injected until the desired operative pressure (P_0) is reached. The gas mixture is stirred, cooled down, and stabilized at the working conditions of temperature (T_0 , typically in the temperature range of 278 to 286 K) and pressure. The gas phase is analysed again by gas chromatography to monitor the initial gas composition.

The temperature needs to be higher than the pure TBAB semi-clathrates equilibrium temperature (without gas), and lower than pure water gas hydrate equilibrium temperature to be sure that gas/TBAB semi-clathrates are formed, and not pure water gas hydrates or pure TBAB semi-clathrates. For example, at a TBAB mass fraction of 0.21, temperature cannot be inferior to 283 K to avoid the formation of pure Type A semi-clathrate (Fig. 1). At a TBAB mass fraction of 0.11, the temperature cannot be inferior to 290 K to avoid the formation of the Type B semi-clathrate.

Once (P_0 , T_0) is stabilized, the stirrer is stopped and the liquid solution ($V_0^L = 1 \text{ dm}^3$) is injected in the reactor

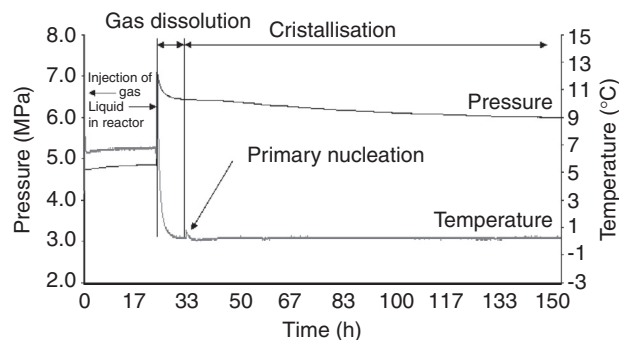


Figure 7

Typical example of the evolution of pressure and temperature during crystallization of pure gas-TBAB semi-clathrates.

by using the HPLC pump. The liquid is composed of a controlled quantity of water ($n_{w,0}^L$ moles) and TBAB ($n_{TBAB,0}^L$ moles). The liquid solution contains also a tracer at a low mole fraction $x_0^{tracer} = 10 \text{ ppm}$ (here LiNO₃). The tracer is not consumed during the crystallization and remains in the liquid phase. Once the liquid phase has been injected in the autoclave, an increase of temperature and pressure is simultaneously observed, firstly because the liquid is at ambient temperature. The temperature increase is also due to the gas compression resulting from the reduction of the gas volume by the liquid. The stirring is started and the pressure decreases due to gas dissolution in the liquid.

After a while (from some minutes to several hours, nucleation being a stochastic phenomenon), crystallization begins. It is accompanied by a sudden increase of temperature (Fig. 7). During crystallization (exothermic process), the pressure decreases due to gas consumption by hydrates and the temperature returns to the operative temperature. After a while, the system reaches the equilibrium (end of crystallization), the pressure and the temperature reach constant values.

Then, we can proceed to gas hydrate dissociation. The temperature of the reactor is heated by steps of 1 K (Fig. 8). During each step, the pressure increases due to gas hydrate dissociation and reaches a constant value which represents the thermodynamic equilibrium.

During the dissociation, at each stage (i) the liquid is sampled and analyzed by refractometry to evaluate the quaternary ammonium concentration, and by ionic chromatography to evaluate the concentration $C^{tracer,i}$.

The gas phase is also sampled and analyzed by gas chromatography.

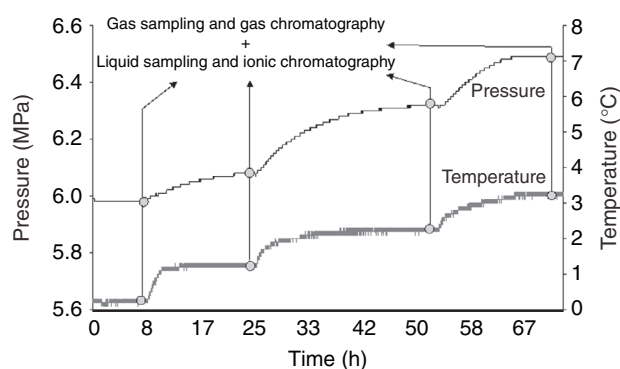


Figure 8

Typical example of the evolution of pressure and temperature during dissociation of pure gas-TBAB semi-clathrates.

6 MASS BALANCES

6.1 Mass Balance for the Gaseous Components

When at given values of the state variables (pressure, temperature, composition), a gaseous, a liquid and a solid hydrate phases are present in the system, the initial quantity of the molecules in the reactor is distributed between these three phases. Thus, in equilibrium, the quantity of gas in the hydrate phase can be determined from a mass balance according to:

$$n_{j,0} = n_j^H + n_j^L + n_j^G \quad (1)$$

In Equation (1), $n_{j,0}$ stands for the initial (total) mole number and n_j^H , n_j^L and n_j^G are the mole numbers of component j ($j = \text{CO}_2, \text{N}_2$) in the hydrate, the liquid and the gas phase, respectively.

The amount of substance in the liquid phase is estimated by means of a corresponding gas solubility data. The mole number in the gas phase is calculated by using an equation of state approach as outlined in the next sections.

The total mole number n^G in the gas phase in any equilibrium state can be calculated by means of the classical Equation (2):

$$Z(T, P, \vec{y}) = \frac{P V}{n R T} \quad (2)$$

For $n \equiv n^G$. In Equation (2), T , P , and V are the temperature, pressure and total volume of the gas phase, respectively, while $\vec{y} = (y_{\text{CO}_2}, y_{\text{N}_2})$, n and R represent the vector of the mole fractions of the components in the mixture,

the total mole number in the gas mixture, and the universal gas constant, respectively. Z is the compressibility factor that can be calculated by means of a suitable Equation of State (EOS), e.g., a classical cubic EOS. In this study, the Soave-Redlich and Kwong (SRK) EOS has been used (parameters from Danesh, 1998).

Each time, the composition of the gas phase is determined by using gas chromatography analysis.

We recall here that the reactor of total inner volume $V_R = 2.51 \text{ dm}^3$ is initially filled with the gaseous components at the initial temperature T_0 and under the initial total pressure P_0 . Therefore, at this stage, the system only consists of a gas phase, being composed of the two gaseous components CO_2 and N_2 . Knowing the temperature, the pressure and the gas composition, the initial mole number, n_0^G , can be calculated as follows:

$$n_0^G = \frac{P_0 V_R}{Z(T, P, \vec{y}_0) R T_0} \quad (3)$$

Equation (2) has also been used to determine the total amount of substance of the gas phase in a state corresponding to the three phase hydrate-liquid-vapour equilibrium. In the latter case, the initial values of the variables are to be replaced by the corresponding measured values in that equilibrium state. Moreover, the volume of the reactor, V_R , has to be replaced by the actual value of the gas volume V^G :

$$V^G = V_R - V^{L+H} \quad (4)$$

where V^{L+H} stands for the volume of the liquid phase and hydrate phase. This volume is assumed to remain equal to the initial liquid volume, (V_0^L), the density of the liquid and hydrate phase being close (1080 kg.m^{-3} for type A hydrate and 1070 kg.m^{-3} for type B hydrate according to Oyama *et al.* (2005), compared to the aqueous densities, measured between 1021 kg.m^{-3} and 1039 kg.m^{-3} according to Darbouret, 2005; Obata *et al.*, 2003; and Belandria *et al.*, 2009). At last, the mole numbers of the respective gaseous component j ($j = \text{CO}_2, \text{CH}_4, \text{N}_2$) in the gas phase, $n_{j,0}^G$ and n_j^G , are respectively given by:

$$n_{j,0}^G = n_0^G y_{j,0} \quad \text{and} \quad n_j^G = n^G y_j \quad (5)$$

6.2 Liquid Phase Volume

The liquid phase contains LiNO_3 as a tracer. Initially the concentration of lithium $[\text{Li}^+]_0$ and the initial volume of liquid V_0^L are known. During the crystallization and dissociation steps, the concentration of lithium is measured

by ion-exchange chromatography after sampling. So, we can calculate the volume of liquid water from a mass balance for the Li⁺ ions:

$$V_0^L [\text{Li}^+]_0 = V^L [\text{Li}^+] \Rightarrow V^L = \frac{V_0^L [\text{Li}^+]_0}{[\text{Li}^+]} \quad (6)$$

where V^L and $[\text{Li}^+]$ are the volume of the liquid aqueous phase and the molar concentration of lithium in this phase.

6.3 Composition of the Liquid Phase

The mass fraction of TBAB in the liquid phase (w_{TBAB}^L) is determined experimentally after on-line sampling of a small amount of the liquid phase and measurement of the index of refraction. In fact, the Index of Refraction (IR) at temperature of 295.15 K is linearly dependent of the mass fraction w_{TBAB}^L in the range of 0 to 0.4, following a correlation given by Darbouret (2005):

$$IR = 1.333 + 0.178 w_{TBAB}^L \quad (7)$$

The mole number n_j^L in the liquid phase (Eq. 9) is calculated in a good approximation by using solubility data of the gas in water (Holder et al., 1988) under the assumption that neither LiNO₃ (due to its low concentration, about 10 ppm), nor TBAB does not affect this solubility. The second hypothesis is done because of the lack of data about the solubility of CO₂ or N₂ in H₂O-TBAB liquid solutions. This is hardly defensible from a fundamental point of view. Thiam et al. (2008) showed that the solubility of CO₂ is decreased by 10 to 15% as the TBAB mass fraction is increased by 10%. But, from a practical point of view, this approximation can be done because the mole number n_j^L is one order of magnitude lower than n_j^H and n_j^G . It does not affect significantly the calculation of n_j^H .

In equilibrium, the equality of the fugacities of the gases in the liquid and the gas phase holds according to:

$$f_j^L(T, P, x_j) = f_j^G(T, P, y_j) \quad (8)$$

Substituting the fugacity in the liquid phase for an extended form of Henry's law (Eq. 10) and expressing the gas phase fugacity in terms of fugacity coefficient n_j^L can be expressed as:

$$n_j^L = \frac{V^L \rho_w^\circ}{M_w} \frac{y_j \phi_j^G P}{K_{H,j}^\infty \exp(P v_j^\infty / RT)} \quad (9)$$

where V^L stands for the volume of the liquid phase in equilibrium, ρ_w° is the density, and M_w is the molar mass of pure water. $v_j^\infty = 32 \text{ cm}^3 \cdot \text{mol}^{-1}$ is the partial molar volume of compound j in water (an average value from Holder et al., 1988). In establishing Equation (9), the activity coefficient of CO₂ in water was in a good approximation neglected and the very good approximations $n_j^L \ll n_w^L$, was applied. $K_{H,j}^\infty$ (Pa⁻¹) represents Henry's constant at saturation pressure of the pure solvent, i.e., at infinite dilution of the gaseous component, which as function of temperature is calculated from the following correlation (Holder et al., 1988):

$$K_{H,j}^\infty(T) [\text{Pa}] = \exp\left(-A - \frac{B}{T}\right) \quad (10)$$

A and B are constants listed in Holder et al. (1988).

6.4 Composition of the Hydrate Phase

After the amounts of substance of compound j in the gas phase n_j^G and in the liquid phase n_j^L have been estimated, the mole number of the gas j in the hydrate phase n_j^H can be derived from Equations (1, 5, 9): the gas encapsulated in the hydrate equals the initial quantity in the feed n_0^G minus the quantities in the gas at step n_j^G and the quantity in the liquid n_j^L .

The amount of water and TBAB in the hydrate phase is assumed to be the part which has been consumed in the liquid phase.

$$n_w^H = n_{w,0}^L - n_w^L = \left(1 - w_{TBAB,0}^L\right) \frac{V_0^L \cdot \rho_0^L}{M_w} - \left(1 - w_{TBAB}^L\right) \frac{V^L \cdot \rho^L}{M_w} \quad (11)$$

$$n_{TBAB}^H = n_{TBAB,0}^L - n_{TBAB}^L = w_{TBAB,0}^L \frac{V_0^L \cdot \rho_0^L}{M_{TBAB}} - w_{TBAB}^L \frac{V^L \cdot \rho^L}{M_{TBAB}} \quad (12)$$

V^L is calculated from Equation (6) and w_{TBAB}^L from Equation (7). M_w and M_{TBAB} are respectively the molar mass of water and TBAB. The density ρ^L of the solution has been measured experimentally by Darbouret (2005) in the temperature range [273.15-297.15] K and the weight fraction of w_{TBAB}^L in the range of [0-0.4]. From these data, Douzet (2011) has proposed a correlation with a precision of 0.1%:

$$\rho^L = 1000 + 99.7 w_{TBAB}^L \quad (13)$$

7 EXPERIMENTAL RESULTS

We present the results of two experiences (*Tab. 6*): one starting with a TBAB mass fraction of 0.21 and an initial CO₂ mole fraction of 0.317, and the other one starting with a TBAB mass fraction of 0.11, and an initial CO₂ mole fraction of 0.665. In both cases, we succeeded in measuring three equilibrium points following the procedure described before. We complete the data with the results of a previous work (*Tab. 7*) at a TBAB mass fraction of 0.40.

Results of this work are compared to equilibrium points at the same initial compositions and similar temperature, but without TBAB (only pure water). With pure water, the equilibrium points are calculated from the GasHyDyn software described in *Herri et al. (2011)*.

Table 8 compares the experimental equilibrium pressure in presence of TBAB to the calculated ones, at the same temperature and gas composition, but for pure water gas hydrate. We can say that the pressure of formation of the semi-clathrate hydrate is considerably decreased, by a factor from 5.4 to 11 for these experiments. It confirms the pressure drop observed on pure gas-TBAB semi-clathrates (*Fig. 3-Fig. 5*).

Figure 9 presents the selectivity of the separation of CO₂ from N₂ during crystallization of semi-clathrate hydrates from TBAB solution. The data from this work are compared to the results from *Duc et al. (2007)*. All the experimental points of this study and from *Duc et al. (2007)* are in the range of temperature [283.4–288.6] K. We have also plotted a reference case

TABLE 6
Experimental results from this study

$w_{TBAB,0}^L$	w_{TBAB}^L	P_{eq} (MPa)	T_{eq} (K)	$n_{CO_2}/(n_{CO_2} + n_{N_2})$			$\frac{z_{CO_2}y_{N_2}}{z_{N_2}y_{CO_2}}$
				Gas y_{CO_2}	Liquid	Hydrate z_{CO_2}	
0.112	0.073	2.5	283.4	0.431	0.243	0.989	118.70
	0.079	2.6	284.4	0.456	0.249	0.984	73.37
	0.091	2.7	285.5	0.50	0.259	0.955	21.22
0.218	0.175	4.9	283.9	0.239	0.556	0.794	12.27
	0.183	5.0	287.5	0.245	0.581	0.764	9.98
	0.189	5.2	288.6	0.254	0.596	0.909	29.34

TABLE 7
Experimental results from *Duc et al. (2007)*

$w_{TBAB,0}^L$	w_{TBAB}^L	P_{eq} (MPa)	T_{eq} (K)	$n_{CO_2}(n_{CO_2} + n_{N_2})$			$\frac{z_{CO_2}y_{N_2}}{z_{N_2}y_{CO_2}}$
				Gas y_{CO_2}	Liquid	Hydrate z_{CO_2}	
0.40	–	0.66	285.15	1	–	1	–
	–	2.01	285.15	0.175	–	0.789	17.63
	–	2.05	285.15	0.174	–	0.783	17.13
	–	3.28	285.15	0.061	–	0.275	5.84
	–	4.44	285.15	0	–	0	–
0.40	–	0.83	286.15	1	–	1	–
	–	2.217	286.15	0.205	–	0.927	49.25
	–	2.257	286.15	0.233	–	0.9182	36.95
	–	3.4	286.15	0.0656	–	0.2851	5.68
	–	4.681	286.15	0	–	0	–

TABLE 8

Comparison of equilibrium pressure P_{eq} at given (T_{eq} , x_{CO_2}) between the semi-clathrate hydrate and the clathrate hydrate

w_{TBAB}^L	T_{eq} (K)	$P_{eq}(w_{TBAB}^L)$ (MPa)	$P_{eq}(w_{TBAB}^L = 0)$ (MPa)	$\frac{P_{eq}(w_{TBAB}^L)}{P_{eq}(w_{TBAB}^L = 0)}$ (-)
0.073	283.4	2.5	13.6	5.4
0.079	284.4	2.6	18.6	7.2
0.091	285.5	2.7	20.8	7.6
0.175	283.9	4.9	24.8	5.0
0.183	287.5	5.0	48.4	9.7
0.189	288.6	5.2	57.2	11.0

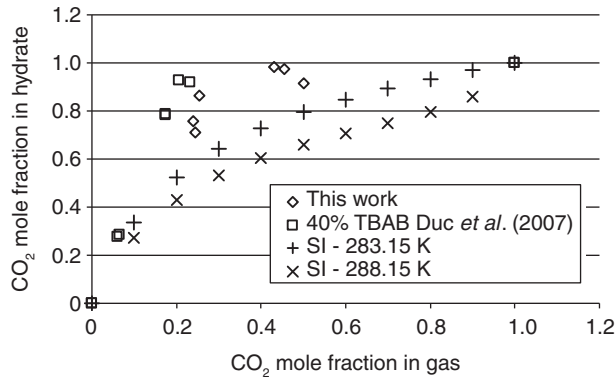


Figure 9

Selectivity of the separation of CO₂ from N₂ during crystallization of semi-clathrate hydrates from TBAB solution, and comparison to the selectivity of clathrate hydrate of structure SI.

consisting in the molar fraction of CO₂ in the SI structure (pure water clathrate hydrate), at two temperatures of 283.15 K and 288.15 K. We can observe an enhancement of the content in CO₂ in the case of the semi-clathrate hydrate of TBAB, even at low molar fraction of CO₂. However, it is observed a difference between the data of this work and the results of [Duc et al. \(2007\)](#). The data from [Duc et al. \(2007\)](#) has been determined with a liquid solution at TBAB mass fraction of 0.4. In our work, the TBAB mass fraction is in the range [0.07-0.18] and could explain the difference. But independently of the differences, it can be underlined that the semi-clathrate hydrate of TBAB has a better affinity to CO₂ in comparison to pure water clathrate hydrate.

For example, at a gas molar fraction of CO₂ around 0.2, the CO₂ molar fraction in the clathrate hydrate is in the range of 0.43 ($T = 288.15$ K) to 0.42 ($T = 283.15$ K) whereas the CO₂ molar fraction in the TBAB semi-clathrate hydrate can be up to 0.93 (from [Duc et al., 2007](#), at a temperature of 286.15 K).

Similarly, at gas molar fraction of CO₂ around the value of 0.5, the CO₂ molar fraction in the clathrate hydrate is in the range 0.66 ($T = 288.15$ K) to 0.79 ($T = 283.15$ K) whereas the CO₂ molar fraction in the TBAB semi-clathrate hydrate can be up to 0.96 (this work) at a temperature of 285.5 K).

8 MODELING

The experimental results of this work show that TBAB decreases drastically the operative pressure, possibly down to the atmospheric pressure. It can be done by adjusting the operative temperature of formation of the Gas-TBAB semi-clathrate hydrate at a temperature close to the temperature of formation of the pure TBAB semi-clathrate hydrate.

[Paricaud \(2011\)](#) proposed a new expression to describe the Gas-TBAB semi-hydrate equilibrium from a model derived from the van der Waals and Platteeuw using θ_j (van der [Waals and Platteeuw, 1959](#))

$$\begin{aligned}
 0 = & \frac{\Delta_{dis} C_m^\ominus (T_{cgr}^{HL_w})}{RT_{cgr}^{HL_w}} + \frac{\Delta_{dis} H_m^\ominus (T_{cgr}^{HL_w})}{RT} \left(1 - \frac{T}{T_{cgr}^{HL_w}} \right) \\
 & + \frac{\Delta_{dis} C_{p,m}^\ominus (T_{cgr}^{HL_w})}{R} \left(1 - \frac{T_{cgr}^{HL_w}}{T} + \ln \frac{T_{cgr}^{HL_w}}{T} \right) \\
 & + \frac{\Delta_{dis} V_m^{ref} (T_{cgr}^{HL_w}, p^\ominus)}{RT} (p - p^\ominus) \\
 & + \ln x_C^{L_w} \gamma_{x,C}^{*,L_w} + \ln x_A^{L_w} \gamma_{x,A}^{*,L_w} + v_w \ln x_w^{L_w} \gamma_w^{L_w} \\
 & - v_i \ln (1 - \theta)
 \end{aligned} \tag{14}$$

γ are the activity coefficients. In this work, a modification of the model approach of [Paricaud \(2011\)](#) is used in which in contrast to the use of the SAFT-VRE equation of state ([Galindo et al., 1999](#)) the electrolyte NRTL model (eNRTL-model) ([Chen et al., 1982](#); [Chen and Evans, 1986](#); [Bollas et al., 2008](#)) is incorporated into the model to describe the liquid phase non-idealities in presence of TBAB ([Kwaterski and Herri, 2011](#))

In Equation (14), $T_{cgr}^{HL_w} = T_{cgr}^{HL_w}(p^\ominus)$ stands for the temperature of the congruent melting point of the semi-clathrate hydrate, *i.e.*, the temperature of the phase transition $\beta \rightarrow L_w \equiv H \rightarrow L_w$ at $p = p^\ominus$.

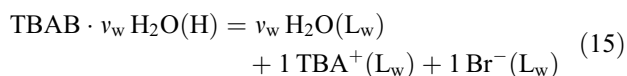
TABLE 9

Reference properties of type A and B TBAB semi-clathrate hydrates

	Type A	Type B
v_w (mole of water/mole of TBAB)	26	38
$T_{cgr}^{HL_w}$ (K)	285.15	283.5
$\Delta_{dis} G_m^\circ(T_{cgr}^{HL_w})$ (J/mol TBAB)	23 804	24 867
$\Delta_{dis} H_m^\circ(T_{cgr}^{HL_w})$ (J/mole TBAB)	146 350	193 060
$\Delta_{dis} C_{p,m}^\circ(T_{cgr}^{HL_w})$	0	0
$\Delta_{dis} V_m^{ref}$ (m ³ /mole TBAB)	−0.00003	−0.00003
Type of free cavity to enclathrate gas	?	5 ¹²
v_i (mole of free cavity/mole of TBAB)	?	2

Numerical values (Tab. 9) for the standard molar quantities, $\Delta_{dis} G_m^\circ(T_{cgr}^{HL_w})$ and $\Delta_{dis} H_m^\circ(T_{cgr}^{HL_w})$ are gained through adjustments of the HL_w-coexistence curves given in Figure 1 (or to the dissociation enthalpies directly if allowable).

If values of the standard molar isobaric heat capacity upon hydrate dissociation are measured directly, they can additionally be used to adjust $\Delta_{dis} C_{p,m}^\circ(T_{cgr}^{HL_w})$. $\Delta_{dis} V_m^{ref}$, evaluated at $T_{cgr}^{HL_w}$ and p° , accounts for the effect of pressure on the melting points for the water + salt binary systems (Paricaud, 2011). Paricaud points out that “different values for $\Delta_{dis} V_m^{ref}(T_{cgr}^{HL_w}, p^\circ)$, $\Delta_{dis} H_m^\circ(T_{cgr}^{HL_w})$, $T_{cgr}^{HL_w}$ and $\Delta_{dis} C_{p,m}^\circ(T_{cgr}^{HL_w})$ should be used for different types of hydrates”. He further reports that v_w should be fixed to its experimental value. v_w is the stoichiometric coefficient of water in the equation of dissociation of a semiclathrate hydrate TBAB · v_w H₂O regarded as a combined chemical reaction and phase equilibrium and can be written as:



The complete modeling of the eNRTL model (Kwaterski and Herri, 2011) has been implemented in the GasHyDyn software (Herri et al., 2011) with the reference parameters from Table 9.

From Equation (14), we can determine analytically the minimum occupancy θ_{\min} which stabilizes the overall structure, independently of the chemical nature of the species in the cavities. It could be a single gas $N_{\text{type g}} = 1$ or a gas mixture ($N_{\text{type g}} > 1$), but the sum of their respective contributions $\sum_{j=1}^{N_{\text{type g}}} \theta_j$ needs to be at least equal to θ_{\min} . The value of θ_{\min} is given in Figure 10 for type B hydrate, as a function of temperature, given as the difference between the operative temperature and $T_{cgr}^{HL_w}$.

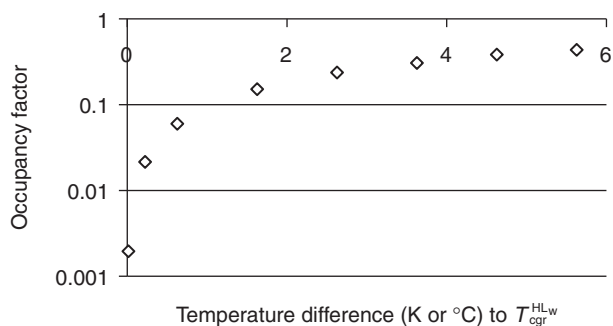


Figure 10

Minimum occupancy factor of cavities 5¹² in the type B semi-clathrate hydrate of TBAB.

From Figure 10, we can determine a correlation to determine the occupancy factor θ_{\min} of the cavities:

$$\theta_{\min} = -3.719 \cdot 10^{-3} \left(T - T_{cgr}^{HL_w} \right)^2 + 9.926 \cdot 10^{-1} \left(T - T_{cgr}^{HL_w} \right) \quad (16)$$

The consequence of Equation (16) is that the minimum gas content in the clathrate structure decreases as the temperature reaches the temperature $T_{cgr}^{HL_w}$ of formation of the pure TBAB semi-clathrate hydrate.

At thermodynamic equilibrium, the content of gas j in the 5¹² cavity of the semi-clathrate hydrate is expressed under the following form (van der Waals and Platteeuw, 1959)

$$\theta_j = \frac{C_{f,j} f_j(T, P)}{1 + \sum_j C_{f,j} f_j(T, P)} \quad (17)$$

θ_j is the occupancy factor ($\theta_j \in [0, 1]$) of the cavities of type 5¹² by the gas molecule $j = \text{CO}_2, \text{N}_2$. $C_{f,j}$ is the Langmuir constant of component j in the cavity 5¹². In this notation, the Langmuir constant is calculated by using a modified Kihara approach (Eq. 18) taking into account the fugacity f as the driving force. It describes the interaction potential between the encaged guest molecule and the surrounding water molecules. f_j is the fugacity of the component.

9 DISCUSSION

9.1 About the Operative Pressure

From correlation (16) and Equation (17), we can see that the operative pressure and gas content in the hydrate

phase follow the same trend, the higher the gas content, the higher the operative pressure. If the operative pressure is lowered, the gas content is decreased also. In terms of process, it implies that we need to handle more hydrate volume to capture a same quantity of CO₂ gas. So the choice of an operative pressure becomes the economic optimum between the minimization of the cost of compression which implies to drop the pressure, and the minimization of the volume of the reactor which implies to increase the pressure.

9.2 About the Hydrate Composition

The results of this work show that TBAB enhances the selectivity of the CO₂ capture (Fig. 9). This enhancement can be explained theoretically from two points of view.

On the one hand, the surrounding of the CO₂ gas molecule encapsulated in the semi-clathrate hydrate structure (Fig. 2) is different from the surrounding in the clathrate hydrate structure because of the vicinity of the TBAB molecule. It affects necessary the Langmuir constant $C_{f,j}$. In fact, the Langmuir constant $C_{f,j}$ is evaluated by assuming a spherically symmetrical cage that can be described by a spherical symmetrical potential (van der Waals and Platteeuw, 1959):

$$C = \frac{4\pi}{kT} \int_0^\infty \exp\left(-\frac{w(r)}{kT}\right) r^2 dr \quad (18)$$

where $w(r)$ is the interaction potential between the structure and the gas molecule according to the distance r between the guest molecule and the water molecules over the structure. If the nature of the structure is modified, the Langmuir constant is modified also, especially if a water molecule at the vicinity of the gas molecules is replaced by a new molecule such as an anion of a halogenide type.

But this hypothesis is not sufficient at explaining the experimental measurements. In fact, from Equation (17), we can write that:

$$\begin{aligned} \frac{\theta_{\text{CO}_2}}{\theta_{\text{N}_2}} &= \frac{z_{\text{CO}_2}}{z_{\text{N}_2}} = \frac{C_{f,\text{CO}_2} f_{\text{CO}_2}(T, P)}{C_{f,\text{N}_2} f_{\text{N}_2}(T, P)} \\ &= \frac{C_{f,\text{CO}_2} Z(T, P, y_{\text{CO}_2}) y_{\text{CO}_2} P}{C_{f,\text{N}_2} Z(T, P, y_{\text{CO}_2}) y_{\text{N}_2} P} \end{aligned} \quad (19)$$

y is the mole fraction of a chemical species in the gas phase, z is the mole fraction of a chemical species in the cavities of the clathrate hydrate structure, and Z is the compressibility factor. The equation becomes:

$$\frac{z_{\text{CO}_2} y_{\text{N}_2}}{z_{\text{N}_2} y_{\text{CO}_2}} = \frac{C_{f,\text{CO}_2}}{C_{f,\text{N}_2}} \quad (20)$$

Because the Langmuir constants (Eq. 18) are only dependent on temperature, the left term of Equation (20) is theoretically constant at a given temperature, but it is not experimentally validated (Tab. 7). So, the semi-clathrate hydrate does not form under thermodynamic equilibrium.

So, if the thermodynamic consideration can not explain the enhancement of the selectivity of the CO₂ in the semi-clathrate hydrate, the other reason is necessary a kinetic one. Based on the fact that clathrates are non-defined component, Herri and Kwaterski (2012) have demonstrated that the composition of the solid is dependent on the relative rates of mass transfers, and on kinetic rates of the reaction of integration of the gaseous molecule in the solid structure under growing, following a modified expression of Equation (17) under the form:

$$\theta_j = \frac{C_{x,j} x_{j,\text{int}} \frac{k_j/G}{1+k_j/G}}{1 + \sum_{j' \in S_g} C_{x,j'} x_{j',\text{int}} \frac{k_{j'}/G}{1+k_{j'}/G}} \quad (21)$$

The Langmuir coefficient is calculated by taking into account the mole fraction x as the driving force. $x_{j,\text{int}}$ is the mole fraction of component j at the vicinity of the growing clathrate hydrate surface. G is the growth rate. k_j is to be regarded as an intrinsic kinetic constant of component j .

The composition of the semi-clathrate hydrate is so fixed by kinetic considerations also, based on the values of the $x_{j,\text{int}}$ which result on a mass balance between:

- the gas to liquid transfer rate that feeds the solution;
- the growth that consumes the gaseous component;
- the affinity of the cavities to adsorb the species, from a thermodynamic point of view ($C_{x,j}$) and a kinetic point of view (k_j).

The solving of the mass balance is given in Herri and Kwaterski (2012) and it implies to couple the mass balance with a population balance to describe the size and the number of crystals in the system.

10 PERSPECTIVES

So, the composition of the gas hydrate is thermodynamic and kinetic dependent. It can be orientated in a favorable direction (*i.e.* the capture of CO₂) by modifying the mass transfer rates to modify the growth rate G , with the use of specific reactor geometries. Also, the selectivity can be modified from a control on the growth constants k_j with the use of kinetic additives. For example, surfactants such as Sodium Dodecyl Sulfate (SDS) present the characteristic to speed up CH₄ hydrate crystallization (Gayet *et al.*, 2005; Tajima *et al.*, 2010; Torre *et al.*, 2011), but not CO₂ hydrate crystallization, while the reverse effect is observed with fluorinated surfactants (Zhong and Rogers, 2000).

CONCLUSION

The present work confirms the possibility to capture CO₂ from a technology based on the crystallization of semi-clathrate hydrate. A first preliminary costing had been previously evaluated by some authors of this paper in [Duc et al. \(2007\)](#) for an application to CO₂ capture in steel making plants. The specificity of the steel making industry is that the flue gases can be very CO₂ rich, from 23% to 25%. We observed that the main part of the cost is due to compressors. In this work, we add new considerations because we understand now that the pressure can be dropped to the atmospheric pressure. In this work, we have shown also experimentally that the selectivity can be orientated in a favorable direction from kinetic considerations. The hydrate composition is 100% CO₂ when the flue gas is above 20% CO₂. It opens the possibility to treat low CO₂ concentrated gases, for example from coal combustion.

ACKNOWLEDGMENTS

This work has been carried out within the ANR CO₂ (French Research Agency) project called SECOHYA and the FP7 European project iCAP (GA n°241393).

REFERENCES

- Arjmandi M., Chapoy A., Tohidi B. (2007) Equilibrium Data of Hydrogen, Methane, Nitrogen, Carbon Dioxide, and Natural Gas in Semi-Clathrate Hydrates of Tetrabutyl Ammonium Bromide, *J. Chem. Eng. Data* **52**, 2153-2158.
- Belandria V., Mohammadi A.H., Richon D. (2009) Volumetric properties of the (tetrahydrofuran + water) and (tetra-*n*-butyl ammonium bromide + water) systems: Experimental measurements and correlations, *J. Chem. Thermodyn.* **41**, 12, 1382-1386.
- Bollas G.M., Chen C.C., Barton P.I. (2008) Refined electrolyte-NRTL model: Activity coefficient expressions for application to multi-electrolyte systems, *AIChE J.* **54**, 6, 1608-1624.
- Brinchi L., Castellani B., Cotana F., Filippini M., Rossi F. (2011) Investigation of a novel reactor for gas hydrate production, Proceedings of the 7th International Conference on Gas Hydrates (ICGH 2011), Edinburgh, Scotland, United Kingdom, 17-21 July.
- Chen C.-C., Britt H.I., Boston J.F., Evans L.B. (1982) Local composition model for excess Gibbs energy of electrolyte systems. Part I: Single solvent, single completely dissociated electrolyte systems, *AIChE J.* **28**, 4, 588-596.
- Chen C.-C., Evans L.B. (1986) A local composition model for the excess Gibbs energy of aqueous electrolyte systems, *AIChE J.* **32**, 3, 444-454.
- Compingt A., Blanc P., Quidort A. (2009) Slurry for Refrigeration Industrial Kitchen Application, Proceedings of 8th IIR Conference on Phase Change Material and Slurries for Refrigeration and Air Conditioning 2009, Karlsruhe, 3-5 June.
- Danesh A. (1998) *PVT and Phase Behaviour of Petroleum Reservoir Fluids*, Elsevier.
- Darbouret M. (2005) Étude rhéologique d'une suspension d'hydrates en tant que fluide frigopporteur diphasique. Résultats expérimentaux et modélisation, *PhD Thesis*, École Nationale Supérieure des Mines de Saint-Étienne, France.
- Darbouret M., Cournil M., Herri J.M. (2005) Rheological study of TBAB hydrate slurries as secondary two-phase refrigerants, *Int. J. Refrig.* **28**, 5, 663-671.
- Davidson D.W. (1973) Clathrate Hydrates, in *Water, a comprehensive treatise; Vol. 2; Water in crystalline hydrates; aqueous solutions of simple nonelectrolytes*, Franks F. (ed.), Plenum Press, New York, pp. 140-146.
- Delahaye A., Fournaison L., Marinhas S., Chatti I., Petitet J.-P., Dalmazzone D., Fürst W. (2006) Effect of THF on equilibrium pressure and dissociation enthalpy of CO₂ hydrates applied to secondary refrigeration, *Industrial Engineering Chemistry Research* **45**, 1, 391-397.
- Deppe G., Tam S.S., Currier R.P., Young J.S., Anderson G.K., Le L.A., Spencer D.F. (2002) A high pressure carbon dioxide separation process in an IGCC Plant, Proceedings of the *Future Energy System and Technology for CO₂ abatement*, Antwerpen, Belgique, 18-19 Nov.
- Deschamps J., Dalmazzone D. (2009) Dissociation enthalpies and phase equilibrium for TBAB semi-clathrates of N₂, CO₂, N₂ + CO₂ and CH₄ + CO₂, *J. Therm. Anal. Calorim.* **98**, 1, 113-118.
- Douzet J. (2011) Conception, construction, expérimentation et modélisation d'un banc d'essai grandeur nature de climatisation utilisant un fluide frigopporteur diphasique à base d'hydrates de TBAB, *PhD Thesis*, École Nationale Supérieure des Mines de Saint-Étienne, France.
- Douzet J., Brantuas P., Herri J.-M. (2011) Cristallisation and flowing of high concentrated slurries of quaternary ammonium semi-clathrates. Application to air conditioning and CO₂ capture, Proceedings of the 7th International Conference on Gas Hydrates (ICGH 2011), Edinburgh, Scotland, United Kingdom, 17-21 July.
- Douzet J., Kwaterski M., Lallemand A., Chauvy F., Flick D., Herri J.M. (2013) Prototyping of a real size air-conditioning system using a tetra-*n*-butylammonium bromide semiclathrate hydrate slurry as secondary two-phase refrigerant - Experimental investigations and modelling, *International Journal of Refrigeration* **36**, 6, 1616-1631.
- Du J., Liang D., Li D. (2010) Experimental Determination of the Equilibrium Conditions of Binary Gas Hydrates of Cyclopentane plus Oxygen, Cyclopentane plus Nitrogen, and Cyclopentane plus Hydrogen, *Industrial Engineering Chemistry Research* **49**, 22, 11797-11800.
- Duc N.G., Chauvy F., Herri J.-M. (2007) CO₂ Capture by Hydrate Crystallization - A Potential Solution for Gas Emission of Steelmaking Industry, *Energy Conversion and Management* **48**, 1313-1322.
- Dyadin Yu.A., Udachin K.A. (1984) Clathrate formation in water-peralkylonium systems, *Journal of Inclusion Phenomena* **2**, 61-72.
- Dyadin Yu.A., Udachin K.A. (1987) Clathrate polyhydrates of peralkylonium salts and their analogs, *Translated from Zhurnal Strukturnoi Khimii* **28**, 3, 75-116, May-June. *J. Structural Chemistry* **28**, 3, 394-432.
- Dyadin Yu.A., Bondaryuk I.V., Aladko L.S. (1995) Stoichiometry of clathrates, *Journal of Structural Chemistry* **36**, 6, 995-1045.
- Fan S.S., Liang D.Q., Guo K.H. (2001) Hydrate Equilibrium Conditions for Cyclopentane and a Quaternary Cyclopentane-Rich Mixture, *J. Chem. Eng. Data* **46**, 4, 930-932.

- Galindo A., Gil-Villegas A., Jackson G., Burgess A.N. (1999) SAFT-VRE: Phase behavior of electrolyte solutions with the statistical associating fluid theory for potentials of variable range, *J. Phys. Chem. B* **103**, 46, 10272-10281.
- Gayet P., Dicharry C., Marion G., Graciaa A., Lachaise J., Nesterov A. (2005) Experimental determination of methane hydrate dissociation curve up to 55 MPa by using a small amount of surfactant as hydrate promotor, *Chemical Engineering Science* **60**, 21, 5751-5758.
- Gibert V. (2006) Ice Slurry, Axima Refrigeration Experience, *7th Conference on Phase Change Materials and Slurries for Refrigeration and Air Conditioning*, Dinan, France, 13-15 Sept.
- Herri J.-M., Bouchemoua A., Kwaterski M., Fezoua A., Ouabbas Y., Cameirao A. (2011) Gas Hydrate Equilibria from CO₂-N₂ and CO₂-CH₄ gas mixtures – Experimental studies and Thermodynamic Modelling, *Fluid Phase Equilibria* **301**, 2, 171-190.
- Herri J.M., Kwaterski M. (2012) Derivation of a Langmuir type of model to describe the intrinsic growth rate of gas hydrates during crystallization from gas mixtures, *Chemical Engineering Science* **81**, 28-37.
- Holder G.D., Zetts S.P., Pradhan N. (1988) Phase Behavior in Systems Containing Clathrate Hydrates: A Review, *Reviews Chemical Engineering* **5**, 1-4, 1-70.
- Herslund, P.J., Thomsen, K., Abildskov, J., von Solms, N., Galfré, A., Brântuas, P., Kwaterski, M., Herri, J.M., Thermodynamic promotion of carbon dioxide-clathrate hydrate formation by tetrahydrofuran, cyclopentane and their mixtures, *International Journal of Greenhouse Gas Control* **17**, 397-410.
- Jeffrey G.A. (1984) Hydrate inclusion compounds, in *Inclusion compounds*, Atwood J.L., Davies J.E.D., MacNicol D.D. (eds), I, 135-190, Academic Press, New York.
- Kamata Y., Oyama H., Shimada W., Ebinuma T., Takeya S., Uchida T., Nagao J., Narita H. (2004) Gas separation method using tetra-*n*-butyl ammonium bromide semi-clathrate hydrate, *Jpn J. Appl. Phys.* **43**, 362-365.
- Kang S.-P., Lee H. (2000) Recovery of CO₂ from Flue Gas Using Gas Hydrate: Thermodynamic Verification through Phase Equilibrium Measurements, *Environ. Sci. Technol.* **34**, 4397-4400.
- Kang S.-P., Lee H., Lee C.-S., Sung W.-M. (2001) Hydrate phase equilibria of the guest mixtures containing CO₂, N₂ and tetrahydrofuran, *Fluid Phase Equilibria* **185**, 1-2, 101-109.
- Kwaterski M., Herri J.M. (2011) Thermodynamic modelling of gas semi-clathrate hydrates using the electrolyte NRTL model, Proceedings of the *7th International Conference on Gas Hydrates (ICGH 2011)*, Edinburgh, Scotland, United Kingdom, 17-21 July.
- Li S., Fan S., Wang J., Lang X., Liang D. (2009) CO₂ capture from binary mixture via forming hydrate with the help of tetra-*n*-butyl ammonium bromide, *Journal of Natural Gas Chemistry* **18**, 1, 15-20.
- Li S., Fan S., Wang J., Lang X., Wang Y. (2010) Clathrate Hydrate Capture of CO₂ from Simulated Flue Gas with Cyclopentane/Water Emulsion, *Chinese Journal of Chemical Engineering* **18**, 2, 202-206.
- Li X.-S., Xu C.-G., Chen Z.-Y., Wu H.-J. (2011) Hydrate-based pre-combustion carbon dioxide capture process in the system with tetra-*n*-butyl ammonium bromide solution in the presence of cyclopentane, *Energy* **36**, 3, 1394-1403.
- Li X.-S., Xu C.-G., Chen Z.-Y., Jing C. (2012) Synergic effect of cyclopentane and tetra-*n*-butyl ammonium bromide on hydrate-based carbon dioxide separation from fuel gas mixture by measurements of gas uptake and X-ray diffraction patterns, *International Journal of Hydrogen Energy* **37**, 1, 720-727.
- Lin W., Delahaye A., Fournaison L. (2008) Phase equilibrium and dissociation enthalpy for semi-clathrate hydrate of CO₂ + TBAB, *Fluid Phase Equilibria* **264**, 1-2, 220-227.
- Linga P., Kumar R., Englezos P. (2007a) Gas hydrate formation from hydrogen/carbon dioxide and nitrogen/carbon dioxide gas mixtures, *Chemical Engineering Science* **62**, 16, 4268-4276.
- Linga P., Kumar R., Englezos P. (2007b) The clathrate hydrate process for post and pre-combustion capture of carbon dioxide, *Journal of Hazardous Materials* **149**, 3, 625-629.
- Linga P., Kumar R., Lee J.-D., Ripmeester J., Englezos P. (2010) A new apparatus to enhance the rate of gas hydrate formation: Application to capture of carbon dioxide, *International Journal of Greenhouse Gas Control* **4**, 4, 630-637.
- Lipkowski J., Komorov V.Y., Rodionova T.V., Dyadin Y.A., Aladko L.S. (2002) The Structure of Tetrabutylammonium Bromide Hydrate, *Journal of Supramolecular Chemistry* **2**, 435-439.
- McMullan R., Jeffrey G.A. (1959) Hydrates of the Tetra-*n*-butyl and Tetra-*i*-amyl Quaternary Ammonium Salts, *Journal of Chemical Physics* **31**, 5, 1231-1234.
- Meunier F., Rivet P., Terrier M.F. (2007) *Froid Industriel*, Ed. Dunod, Paris.
- Mizukami T. (2010) Thermal Energy Storage system with clathrate hydrate slurry, *Keio University "Global COE Program" International Symposium, Clathrate Hydrates and Technology Innovations, Challenges Toward a Symbiotic Energy Paradigm*, Yokohama, Japan 15, March.
- Mohammadi A.H., Richon D. (2009) Phase equilibria of clathrate hydrates of methyl cyclopentane, methyl cyclohexane, cyclopentane or cyclohexane + carbon dioxide, *Chemical Engineering Science* **64**, 24, 5319-5322.
- Mohammadi A.H., Richon D. (2010) Clathrate hydrate dissociation conditions for the methane + cycloheptane/cyclooctane + water and carbon dioxide + cycloheptane/cyclooctane + water systems, *Chemical Engineering Science* **65**, 10, 3356-3361.
- Mohammadi A.H., Richon D. (2011) Phase equilibria of binary clathrate hydrates of nitrogen + cyclopentane/cyclohexane/methyl cyclohexane and ethane + cyclopentane/cyclohexane/methyl cyclohexane, *Chemical Engineering Science* **66**, 20, 4936-4940.
- Nakajima M., Ohmura R., Mori Y.H. (2008) Clathrate Hydrate Formation from Cyclopentane-in-water emulsion, *Ind. Eng. Chem. Res.* **47**, 22, 8933-8939.
- Ogoshi H., Matsuyama E., Miyamoto H., Mizukami T. (2010) Clathrate Hydrate Slurry, CHS Thermal Energy Storage System and Its Applications, Proceedings of *2010 International Symposium on Next-generation Air Conditioning and Refrigeration Technology*, Tokyo, Japan, 17-19 Feb.
- Obata Y., Masuda N., Joo K., Katoh A. (2003) Advanced Technologies Towards the New Era of Energy Industries, *NKK Tech. Rev.* **88**, 103-115.
- Oyama H., Shimada W., Ebinuma T., Kamata Y. (2005) Phase diagram, latent heat, and specific heat of TBAB semiclathrate hydrate crystals, *Fluid phase Equilib.* **234**, 1-2, 131-135.
- Oyama H., Ebinuma T., Nagao J., Narita H. (2008) Phase Behavior of TBAB Semiclathrate Hydrate Crystal under several Vapor Components, Proceedings of the *6th International Conference on Gas Hydrates (ICGH 2008)*, Vancouver, British Columbia, Canada, 6-10 July.
- Paricaud P. (2011) Modeling the Dissociation Conditions of Salt Hydrates and Gas Semiclathrate Hydrates: Application to Lithium Bromide, Hydrogen Iodide, and Tetra-*n*-butylammonium Bromide + Carbon Dioxide Systems, *J. Phys. Chem. B* **115**, 2, 288-299.

- Riesco N., Trusler J.P.M. (2005) Novel optical flow cell for measurements of fluid phase behavior, *Fluid Phase Equilibria* **228-229**, 233-238.
- Sabil K.M., Witkamp G.-J., Peters C.J. (2010) Phase equilibria in ternary (carbon dioxide + tetrahydrofuran + water) system in hydrate-forming region: Effects of carbon dioxide concentration and the occurrence of pseudo-retrograde hydrate phenomenon, *Journal of Chemical Thermodynamics* **42**, 1, 8-16.
- Sato K., Tokutomi H., Ohmura R. (2013) Phase Equilibrium of Ionic Semiclathrate Hydrates formed with Tetrabutylammonium Bromide and Tetrabutylammonium Chloride, *Fluid Phase Equilibria* **337**, 115-118.
- Seo Y.-T., Kang S.-P., Lee H. (2001) Experimental determination and thermodynamic modeling of methane and nitrogen hydrates in the presence of THF, propylene oxide, 1,4-dioxane and acetone, *Fluid Phase Equilibria* **189**, 1-2, 99-110.
- Seo Y., Kang S.-P., Lee S., Lee H. (2008) Experimental Measurements of Hydrate Phase Equilibria for Carbon Dioxide in the Presence of THF, Propylene Oxide, and 1,4-Dioxane, *J. Chem. Eng. Data* **53**, 2833-2837.
- Shimada W., Ebinuma T., Oyama H., Kamata Y., Takeya S., Uchida T., Nagao J., Narita H. (2003) Separation of Gas Molecule Using Tetra-*n*-butyl Ammonium Bromide Semi-Clathrate Hydrate Crystals, *Jpn J. Appl. Phys.* **42**, L129-L131.
- Shimada W., Ebinuma T., Oyama H., Kamata S., Narita H. (2005a) Free-growth forms and growth kinetics of tetra-*n*-butyl ammonium bromide semi-clathrate hydrate crystals, *J. Cryst. Growth* **274**, 246-250.
- Shimada W., Shiro M., Kondo H., Takeya S., Oyama H., Ebinuma T., Narita H. (2005b) Tetra-*n*-butylammonium bromide-water (1/38), *Acta Cryst.* **C61**, o65-o66.
- Sloan E.D. (1998) *Clathrate Hydrates of Natural Gases*, 2nd ed., Marcel Dekker, New York.
- Sloan E.D., Koh C.A. (2008) *Clathrate hydrates of natural gases*, 3rd ed., CRC Press, Boca Raton.
- Spencer D.F. (1997) Methods of selectively separating CO₂ from a multicomponent gaseous stream, US Patent 5700311.
- Spencer D.F. (2000) Methods of selectively separating CO₂ from a multicomponent gaseous stream, US Patent 6106595.
- Suginaka T., Sakamoto H., Iino K., Sakakibara Y., Ohmura R. (2013) Phase Equilibrium for Ionic Semiclathrate Hydrate Formed with CO₂, CH₄, or N₂ plus Tetrabutylphosphonium Bromide, *Fluid Phase Equilibria* **344**, 108-111.
- Tajima H., Yamasaki A., Kiyono F. (2004) Energy consumption estimation for greenhouse gas separation processes by clathrate hydrate formation, *Energy* **29**, 11, 1713-1729.
- Tajima, H., Kiyono, F., Yamasaki, A. (2010) HYPERLINK "/full_record.do?product=UA&search_mode=GeneralSearch&qid=2&SID=Z1iFau3bbGfvrwrcdbBP&page=1&doc=5". Direct Observation of the Effect of Sodium Dodecyl Sulfate (SDS) on the Gas Hydrate Formation Process in a Static Mixer, *Energy & Fuels* **24**, 432-438.
- Takao S., Ogoshi H., Matsumoto S. (2001) Air conditioning and thermal storage systems using clathrate hydrate slurry, US Patent 6560971 B2.
- Takao S., Ogoshi H., Matsumoto S. (2002) Air conditioning and thermal storage systems using clathrate hydrate slurry, US Patent 083720 A1.
- Takao S., Ogoshi H., Fukushima S., Matsumoto H. (2004) Thermal storage medium using a hydrate and apparatus thereof, and method for producing the thermal storage medium, US Patent 20050016200.
- Thiam A., Bouchemoua A., Chauvy F., Herri J.-M. (2008) Gas Hydrates Crystallization from CO₂-CH₄ gas mixtures: Experiments and modelling, Proceedings of the 6th International Conference on Gas Hydrates (ICGH 2008), Vancouver, British Columbia, Canada, 6-10 July.
- Tohidi B., Danesh A., Todd A.C., Burgass R.W., Østergaard K.K. (1997) Equilibrium data and thermodynamic modelling of cyclopentane and neopentane hydrates, *Fluid Phase Equilibria* **138**, 1-2, 241-250.
- Torre J.P., Dicharry C., Ricaurte M., Daniel-David D., Broseta D. (2011) CO₂ capture by hydrate formation in quiescent conditions: In search of efficient kinetic additives, *Energy Procedia* **4**, 621-628.
- van der Waals J.H., Platteeuw J.C. (1959) Clathrate solutions, *Adv. Chem. Phys.* **2**, 1-57.
- Xu C.G., Li X.S., Lv Q.N., Chen Z.Y., Cai J. (2012) Hydrate-based CO₂ (carbon dioxide) capture from IGCC (integrated gasification combined cycle) synthesis gas using bubble method with a set of visual equipment, *Energy* **44**, 358-366.
- Yang H., Fan S., Lang X., Yang Y. (2011) Phase Equilibria of Mixed Gas Hydrates of Oxygen + Tetrahydrofuran, Nitrogen + Tetrahydrofuran, and Air + Tetrahydrofuran, *Journal of Chemical and Engineering Data* **56**, 11, 4152-4156.
- Zhang J.S., Lee J.W. (2009a) Equilibrium of Hydrogen + Cyclopentane and Carbon Dioxide + Cyclopentane Binary Hydrates, *Journal of Chemical and Engineering Data* **54**, 2, 659-661.
- Zhang J.S., Lee J.W. (2009b) Enhanced Kinetics of CO₂ Hydrate Formation under Static Conditions, *Industrial Engineering Chemistry Research* **48**, 13, 5934-5942.
- Zhang J., Yedlapalli P., Lee J.W. (2009) Thermodynamic analysis of hydrate-based pre-combustion capture of CO₂, *Chemical Engineering Science* **64**, 22, 4732-4736.
- Zhong Y., Rogers R.E. (2000) Surfactant effects on gas hydrate formation, *Chemical Engineering Science* **55**, 19, 4175-4187.

Manuscript accepted in October 2013

Published online in April 2014

Copyright © 2014 IFP Energies nouvelles

Permission to make digital or hard copies of part or all of this work for personal or classroom use is granted without fee provided that copies are not made or distributed for profit or commercial advantage and that copies bear this notice and the full citation on the first page. Copyrights for components of this work owned by others than IFP Energies nouvelles must be honored. Abstracting with credit is permitted. To copy otherwise, to republish, to post on servers, or to redistribute to lists, requires prior specific permission and/or a fee: request permission from Information Mission, IFP Energies nouvelles, revueogst@ifpen.fr.